APPLICATION OF THE PHYSICAL OPTICS METHOD TO IMPEDANCE WEDGE DIFFRACTION PROBLEM

A THESIS SUBMITTED TO
THE GRADUATE SCHOOL OF NATURAL AND APPLIED SCIENCES OF
ÇANKAYA UNIVERSITY

BY
NEBAHAT YAĞMUR KÜÇÜKKARA

IN PARTIAL FULFILLMENT OF THE REQUIREMENTS
FOR
THE DEGREE OF MASTER OF SCIENCE
IN
ELECTRONIC AND COMMUNICATION ENGINEERING

JANUARY 2021

ABSTRACT

APPLICATION OF THE PHYSICAL OPTICS METHOD TO IMPEDANCE WEDGE DIFFRACTION PROBLEM

KÜÇÜKKARA, Nebahat Yağmur

M.S.c., Department Of Electronic And Communication Engineering

Supervisor: Prof. Dr. Yusuf Ziya UMUL

In this thesis, the scattered electric field by impedance half-plane and a perfect electric conducting (PEC) wedge will be investigated by using the method of physical optics (PO). The physical optics method is enlarged for the wedge diffraction problem. The integral of physical optics, which consists of the incident and reflected scattered waves, is considered in the diffraction problem of plane waves by a PEC half-plane. The expression of scattered electric fields based on the physical optics method are derived for a PEC wedge. In addition, the solutions of physical optics integral are examined for the regions of a PEC wedge and surface wave fields. The integrals are evaluated by using the stationary phase and edge point methods. The uniform diffracted waves are obtained by the asymptotic evaluation of the physical optics integral. The behaviours of the scattered electric field, the incident and reflected physical optics integrals, total, total geometric optics, diffracted, and uniform diffracted field were plotted and analyzed numerically. The results were also compared with the literature.

Keywords: Physical Optics, Wedge Diffraction, Impedance Surfaces.

ÖZ

EMPEDANS KAMA KIRINIM PROBLEMLERİNDE FİZİKSEL OPTİK METODUN UYGULANMASI

KÜÇÜKKARA, Nebahat Yağmur

Yüksek Lisans, Elektronik ve Haberleşme Mühendisliği Anabilim Dalı

Tez Yöneticisi: Prof. Dr. Yusuf Ziya UMUL

Bu tezde, empedans yarı düzlemi ile saçılan elektrik alanı ve mükemmel bir elektrik iletken (PEC) kama, fiziksel optik (PO) yöntemi kullanılarak incelenecektir. Kama kırınım problemi için fiziksel optik yöntemi genişletilmiştir. Gelen ve yansıyan saçılan dalgalardan oluşan fiziksel optiğin integrali, bir mükemmel iletken yarı düzlemi tarafından düzlem dalgalarının kırınım probleminde ele alınır. Fiziksel optik yöntemine dayalı saçılan elektrik alanlarının ifadesi, bir mükemmel iletken kama için türetilmiştir. Ek olarak, bir mükemmel kamanın bölgeleri ve yüzey dalga alanları için fiziksel optik integralinin çözümleri incelenmiştir. İntegraller, stasyonel faz ve köşe nokta metodu kullanılarak hesaplanmıştır. Düzgün kırınımlı dalgalar, fiziksel optik integralinin asimptotik değerlendirilmesiyle elde edilir. Saçılan elektrik , gelen ve yansıyan fiziksel optik integraller, toplam, toplam geometrik optik, kırınımlı ve tekdüze kırınımlı alanların grafikleri çizdirilmiş ve sayısal olarak analiz edilmiştir. Sonuçlar ayrıca literatür ile karşılaştırılmıştır.

Anahtar Kelimeler: Fiziksel Optik, Kama Kırınımı, Empedans Yüzeyler.

ACKNOWLEDGEMENTS

I would like to thank my sincere gratitude to my supervisor Prof. Dr. Yusuf Ziya UMUL for all his help, supervision, special guidance, suggestions, and encouragement through the improvement of this thesis. It was a great chance and opportunity to work with him.

My special thanks are for my family. I am deeply grateful to them for their encouragement, trust and endless support in all conditions.

TABLE OF CONTENTS

LIST OF FIGURES

LIST OF ABBREVIATIONS

PO	Physical Optics
GO	Geometrical Optics
HF	High Frequency
EP	Edge Point
PEC	Perfect Electric Conducting
MTPO	Modified Theory Of Physical Optics
RSB	Reflected Shadow Boundary
ISB	Incident Shadow Boundary

CHAPTER 1

INTRODUCTION

1.1. Background

The Physical Optics (PO) is a high frequency technique, which is based on the determination of the equivalent current densities induced on the surface of an illuminated perfect electric conductor (PEC) plane [3,6]. In 1913, The PO Method was put forward by Mcdonald [5]. Because the conditions of both incident and reflection have a property in high frequenciens, the related approach is valid for the wedge diffraction problem. Many areas of the electromagnetic theory use this method. For example, The PO Method is benefited from evaluating approximate uniform diffraction coefficients for impedance surfaces. The PO is used to determine the surface current density that causes electromagnetic scattering. So, it is one of the most widely used methods in the literature. On the other hand, due to the its deficiencies, the usage of this method is limited [1]. One of these disadvantages is explained that the edge point contributions of the PO integrals give rise to the erroneous edge diffracted waves and the erroneous evaluation of the edge diffracted fields. There have been approachs by some authors in the literature to do away with this disadvantage. Umul did away with this deficiency of PO in its mathematical structure through three axioms bottomed on the diffraction theory. He expressed that the exact diffracted waves are maintained by the asymptotic evaluation of the modified theory of physical optics (MTPO). At the same time, this method for wedges and impedances surfaces is improved by Umul [10,12]. A canonical attempt for the coated conducting geometries is represented by impedance surfaces [12]. Maliuzhinets was found the first solution of an impedance wedge problem and the total scattered field with a spectrum integral of plane waves, which involves an unknown weight function

[14]. The weight function is obtained with respect to the situations of boundary, radiation, and edge. The zero current density in the shadow region of the scatterer is defined by another disadvantage of PO [1]. Hence, the merely one illuminated face of a wedge diffraction problem is symbolized by PO as a half-plane problem. This problem based on the construction of MTPO integrals is researched by Umul for a conducting half-plane. He indicated that according to PO integrals, it is likely to explain the shadow currents for a conducting half-plane.

The aim of this thesis is to show both illuminated and shadow regions of PEC half-plane and the wedge diffraction with the high frequency (HF) methods. It is also aimed to obtain the scattered electric field expression in the infinite plane problem as a PO integral through a wedge. The scattered electric field expression is obtained in the infinite plane problem [2], but it is not included in the literature. In chapter 3.4, the scattered electric field in the half-plane is converted to the wedge form with the help of the geometry of wedge and region division for GO and diffracted fields, i.e., Fig. 4. Two cases of soft and hard surfaces will be considered for PO integrals.

Geometrical Optics is an approximate high frequency method because of determining wave propagation for incident, reflected, and refracted fields. Because geometrical optics (GO) uses the electromagnetic waves which circulate in ray concepts at high frequencies, it is generally referred to ray optics. According to the PO technique, incident and reflected fields on the object is determined by the geometrical optics. Stutzman expressed that because the equations obtained from PO for the scattered field from a conducting body degrade to the equations of GO in the high frequency (HF) limit, frequently, the concepts of PO can be accepted a little more general than geometrical optics. Practically, it is supposed that PO field at the surface of the scattering surface is the GO surface field. This condition means that the scattering takes place at each point on the illuminated side of the scatterer as though there were an infinite tangent plane at that point as the field at the scattering surface is zero over the shadow zone of the scatterer [8].

In addition, Matlab codes are benefited from Ref. [13]. Since the PO expressions (i.e., x', R and β), which are used in the Matlab code, are the same, the same parameters are defined in the Matlab code in this thesis. The mathematical structure of the PO integrals is also significant point [1]. The conversion of the integrand of the scattered electric field equation in an impedance to the wedge diffraction form will give more comprehension concerning the structure of the PO method. The integrand is also consisted of the incident and reflected waves to reproduce the wedge diffracted waves. Furthermore, the obtained integrals will be calculated asymptotically and compared numerically. All obtained fields during this thesis will be analyzed numerically in the chapter 4, which is called the numerical parts, by using MATLAB.

The time factor of $\exp(j\omega t)$ is compressed and supposed throughout this thesis where ω is the angular frequency.

1.2. Objectives Of The Study

The primary goal of this study is to switch from the dark situations in wedge surfaces using the PO method and its application. The illuminated situations can be applied using the PO method in the wedge surfaces, whereas the PO method cannot be applied in the dark situations. Hence, the obtained integral expression of the scattered electric field is generalized for the PEC surfaces. This expression is used for obtaining the incident PO and reflected PO equations, the investigation of the wedge diffraction problem. In addition, the contribution of the diffracted field to the scattered electric field for diverse geometries such as half-plane with the impedance boundary conditions and wedge is also examined. In some applications, asymptotic and uniform scattered electric field expressions are compared. All these fields statements are examined numerically.

1.3. Organization Of The Thesis

Five chapters are involved in this thesis. All the essential information about the integral of scattered electric field to the forms of PO, GO, and the wedge, methods used for the incident and reflected fields, and numerical analysis of these fields are explained in the diverse geometries. To explain these chapters briefly;

Chapter 1 involves an introduction to the literature review about this thesis, organization and objectives of this thesis.

Chapter 2 is an introduction of the HF methods, which will be used in this thesis. These methods involves the methods of physical optics and geometrical optics.

Chapter 3 includes line integral representation of the scattered electric field and generalization process, the incident PO and reflected PO equations for an impedance half-plane, the conversion of the scattered electric field to GO form in an impedance half-plane, the conversion of scattered field equation in an impedance to the wedge form, and comparison of the asymptotic and uniform scattered electric field.

In Chapter 4, The obtained graphs using MATLAB will be plotted by comparing them with each other, numerically.

In Chapter 5, the conclusion part is involved.

CHAPTER 2

HIGH FREQUENCY METHODS

2.1. Physical Optics (PO)

The geometry in Fig. 1 is taken into account [7]. Scattered fields from S_1 surface are defined as the perfectly conducting surface (PEC surface) and the aperture part, respectively. A surface current on S_1 is caused by the incident waves. The reflected diffracted fields in PO theory are given by the integration of this current. However, this condition will not contain information about incident diffracted fields. According to the surface equivalence theorem, the fields on an imaginary closed surface are obtained by accommodating the electric and magnetic current densities over the closed surface that satisfy the boundary conditions [3]. Equivalent currents can be explained on the aperture according to this theorem. Radiated fields, which are called the incident and reflected diffracted waves, can be obtained by integrating the equivalent currents on S_1 [7].

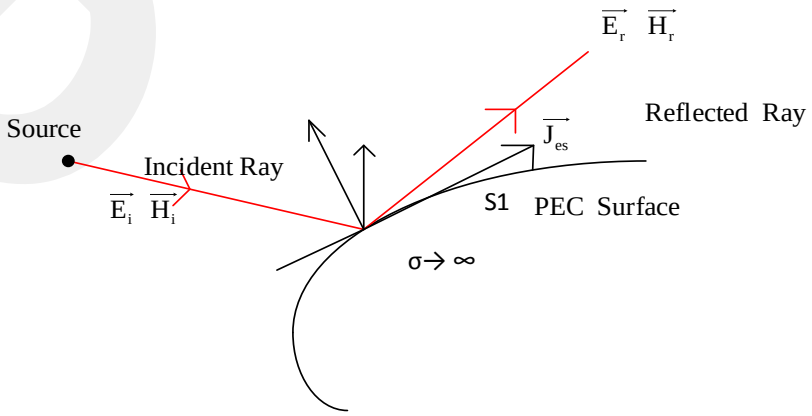

Fig. 1. The geometry of scattered fields from PEC surface

According to Fig. 1, $\overrightarrow{J_{es}}$ is defined as the induced current by the incident ray. This surface current can be defined as

$$\overrightarrow{J_{PO}} = \vec{n} \times \overrightarrow{H_T}|_S \tag{2.1}$$

and,

$$\overrightarrow{J_{PO}} = 0 \tag{2.2}$$

for both the enlightened region and shadow region in a perfectly conducting surface , respectively, where $\overrightarrow{H_T}$ is the total magnetic field on the PEC surface, and $\vec{n}$ is the unit normal vector on the illuminated part of the region as shown in Fig. 2. According to the boundary conditions of any scatterer's surface, this current is formed mathematically. Scattered fields consist of geometrical optics fields which are defined as the fields of incident $\left(\overrightarrow{E_i}\right)$ and reflected $\left(\overrightarrow{E_r}\right)$, and diffracted fields $\left(\overrightarrow{E_d}\right)$.

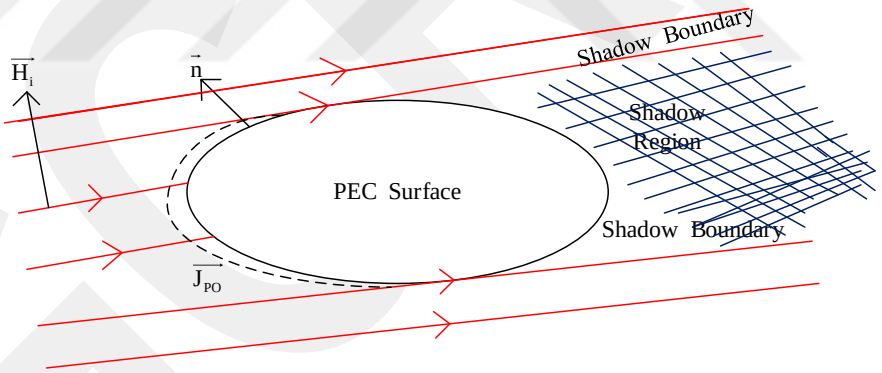

Fig. 2. The geometry of enlightened and shadow regions of PO on the PEC surface

Because of the image theory, when the PEC surface is altered by equivalent currents in free space, the tangential component of H at a perfect conductor are twice those from the same source [8]. Hence, Eq. (2.1) can be rewritten as

$$\overrightarrow{J_{PO}} = 2\vec{n} \times \overrightarrow{H_i} \ . \tag{2.3}$$

Suppose that the incident field phase is to be zero at the reference plane. The total scattering PO field in the far field assumptions can be obtained as

$$\overrightarrow{E_S}^{PO} \cong -j\omega\vec{A} \tag{2.4}$$

or

$$\overrightarrow{E_S}^{PO} = -\frac{j\omega\mu_0}{4\pi}\iint_S 2\vec{n}\times\overrightarrow{H_i}|_S \frac{e^{-jkR}}{R}dS' \tag{2.5}$$

where $\vec{A}$ is defined as the magnetic vector potential. In order to find the magnetic vector potential, using the surface current, POs scattering integral can be written as

$$\vec{A} = \frac{\mu_0}{4\pi}\iint_S 2\vec{n}\times\overrightarrow{H_i}|_{S'} GdS' \tag{2.6}$$

where the integral is expressed as the surface. The term G, which is called the free space Green's function, is equal to $\left(\frac{e^{-jkR}}{R}\right)$ where minus sign in the exponential term corresponding the waves is propagating in the outward direction, and R is called the distance between the source and observation point. The Green's function consists of the information of phase and magnitude alterations apart from the source.

When there are no obstacles in space, the geometry in Fig. 3 is considered [2].

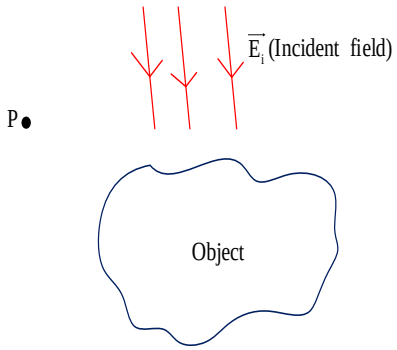

Fig. 3. No obstacles in space

According to Fig. 3, $\overrightarrow{E_T}$, which is the measured field at point P (observation point), is formed as a result of the interaction of the incident field with the object. $\overrightarrow{E_T}$ is written as

$$\overrightarrow{E_T} = \overrightarrow{E_i} + \overrightarrow{E_S} \tag{2.7}$$

where $\overrightarrow{E_i}$ is defined as the incident field and $\overrightarrow{E_S}$ is defined as the scattered field. Using the equation of $\overrightarrow{E_S}$, $\overrightarrow{E_T}$ can be rewritten as

$$\overrightarrow{E_T} = \overrightarrow{E_i} - \frac{j\omega\mu_0}{4\pi}\iint_{S'} 2\vec{n}\times\overrightarrow{H_i}|_S \frac{e^{-jkR}}{R} dS' . \tag{2.8}$$

In this manner, it is understood that any field within the PO field does not exist in space. Keep in mind the equation of the scattered field depends on the frequency in contrast to the expression of geometrical optics does not depend on the frequency. Therefore, it may be assumed that a more exact approximation for the scattered field is provided by physical optics.

2.2. Geometrical Optics (GO)

Geometrical optics, or ray optics was originally developed to analyze the propagation of light where the frequency is sufficiently high that the wave nature of light is not to be considered [8]. Geometrical optics can be improved by the transport of energy from one point to another without any reference in order to control the transfer environment is particle or wave in nature.

Using the canonical geometry of Fig. 4, the solutions of PO fields can be separated from geometrical optics (i.e., incident and reflected), diffracted (i.e., incident and reflected) for the PEC wedge and surface wave fields [3]. Surface waves have to be contained since the wedge has impedance surfaces.

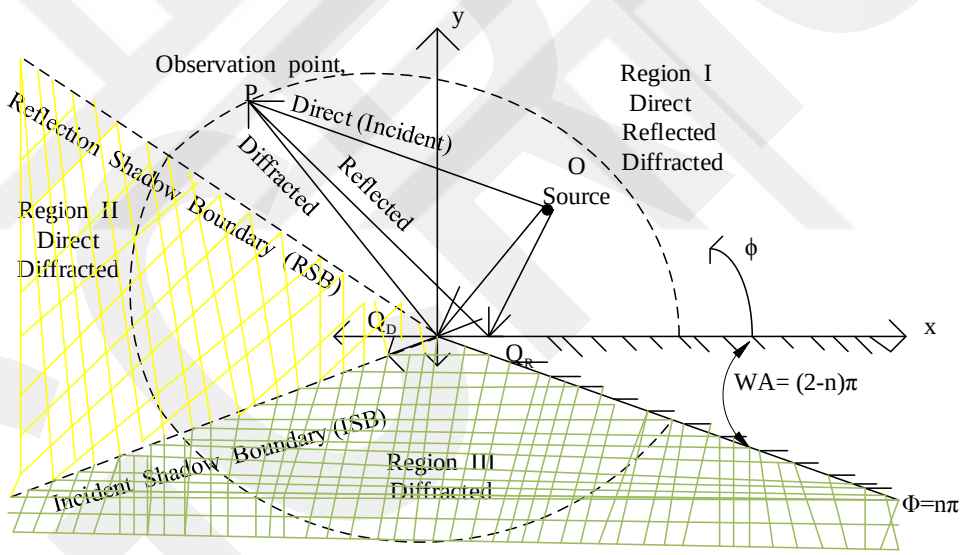

Fig. 4. The geometry of wedge and region division for GO and diffracted fields

According to Fig. 4, the geometry is outside the wedge (i.e., $(0 \le \phi \le n\pi)$), which has been subdivided into three different field regions (i.e., Region I, Region II, Region III) [3]. WA, which is called the two dimensional electric conducting wedge of included angle, is equal to $[(2-n)\pi]$ radians where n, FN, is the wedge angle factor, and $(n\pi)$, ψ, is the outer angle of the wedge.

Using the geometrical coordinates of Fig. 4, the geometrical optics fields can be contributed that Region I, which is called Direct Reflected Diffracted, is expressed as $(0 < \phi < \pi - \phi_0)$, Region II, which is called Direct Diffracted, is expressed as $(\pi - \phi_0 < \phi < \pi < \phi_0)$, and Region III, which is called Diffracted, is expressed as $(\pi + \phi_0 < \phi < n\pi)$. With these fields, it is clear that discontinuous in the field will be modeled along the RSB (i.e., $(\phi = \pi - \phi_0)$) separating regions I and II, and along the ISB (i.e., $(\phi = \pi + \phi_0)$) separating regions II and III, and there are no field in region III (i.e., Shadow Region).

CHAPTER 3

THEORY

3.1. THE BASIS OF THE INFINITE PLANE PROBLEM

An infinite conducting half plane, which is located at $y = 0$, $x \in (0, \infty)$, and $z \in (-\infty, \infty)$ is considered [2]. An incident plane wave $\left(\overrightarrow{E_i}\right)$ of $\overrightarrow{e_z}\overrightarrow{E_0}\exp\left[\,jk\left(x\cos\phi_0 + y\sin\phi_0\right)\right]$ is illuminating the infinite conducting half plane, and an incident magnetic plane wave $\overrightarrow{H_i}$ defines as the equation of $-\frac{\overrightarrow{E_0}}{Z_0}\left(\sin\phi_0\,\overrightarrow{e_x} - \cos\phi_0\,\overrightarrow{e_y}\right)\exp\left[\,jk(x\cos\phi_0 + y\sin\phi_0)\right]$. $\overrightarrow{e_z}$ expresses the propagation direction of incident plane wave, $\overrightarrow{E_0}$ defines as the complex amplitude of the electric or magnetic field, Z_0 is the a physical constant relating the magnitudes of the electric and magnetic fields of electromagnetic radiation travelling through free space [4], ϕ_0 is the angle of incidence, and k is the wave number [1]. Boundary condition between total electric field and total magnetic field on the infinite conductor half plane can be written as

$$n \times \left(n \times \overrightarrow{E_T}\right)|_s = -Zn \times \overrightarrow{H_T}|_s \,. \tag{3.1}$$

Eq. (3.1) can be rearranged as

$$\overrightarrow{E_Z}|_{y=0} = -Z\overrightarrow{H_X}|_{y=0} \,. \tag{3.2}$$

Eq. (3.2) is the boundary condition to be used here. The Helmholtz Equation is used to be solve this boundary condition [2]. The Helmholtz Equation can be written as

$$\nabla^2\overrightarrow{E_Z} + k^2\overrightarrow{E_Z} = 0. \tag{3.3}$$

The expression of $\overrightarrow{E_Z}$ in Eq. (3.3) depends on the parameters of x and y, and it can be showed that

$$\frac{d^2\overrightarrow{E_Z}}{dx^2}+\frac{d^2\overrightarrow{E_Z}}{dy^2}+k^2\overrightarrow{E_Z}=0. \tag{3.4}$$

Since The Helmholtz Equation is equal to zero, that is, it is homogeneous, this equation is solved by The Method Of Separation Of Variables. This method can be written as

$$\overrightarrow{E_Z}(x,y)=X(x)Y(y). \tag{3.5}$$

Eq. (3.5) can be rearranged as

$$X^{"}Y+XY^{"}+k^2XY=0. \tag{3.6}$$

Eq. (3.6) can be divided by XY, and so, the following equation can be obtained as

$$\frac{X^{"}}{X}+\frac{Y"}{Y}+k^2=0. \tag{3.7}$$

The wave number in the opposite direction x $\left(-k_x{}^2\right)$ and the wave number in the opposite direction y $\left(-k_y{}^2\right)$ can be obtained in Eq. (3.7). The wave number in the opposite direction x is equal to $\frac{X^{"}}{X}$, and the wave number in the opposite direction y is equal to $\frac{Y^{"}}{Y}$. The reason why $\left(k_x{}^2\right)$ and $\left(k_y{}^2\right)$ are negative; this is because they are not hyperbolic. Hyperbolic expressions appear in electrostatics and they are phase and amplitude. Therefore, the constants of $\left(k_x{}^2\right)$ and $\left(k_y{}^2\right)$ must be negative.

The wave number, k, can be shown as

$$k=\sqrt{k_x{}^2+k_y{}^2}\ . \tag{3.8}$$

By taking the combination of the axes, Eq. (3.5) can be written as

$$\overrightarrow{E_Z}(x,y)=\left[Ae^{jk_x x}+Be^{-jk_x x}\right].\left[Ce^{jk_y y}+De^{-jk_y y}\right]. \quad (3.9)$$

When Eq. (3.9) is edited, the general solution can be obtained as

$$\overrightarrow{E_Z}=Ae^{-j(k_x x+k_y y)}+Be^{-j(k_x x-k_y y)}+Ce^{j(k_x x-k_y y)}+De^{j(k_x x+k_y y)}\ . \quad (3.10)$$

The equation providing the expressions which A, B and C coefficients are existed in Eq. (3.10) is shown as $E|_{x=0}=0$. The coefficient D is $\overrightarrow{E_0}$. The representations of parameters of k_x and k_y in terms of k are defined as $(k\cos\phi_0)$ and $(k\sin\phi_0)$, respectively. The expression of D coefficient is the incident plane wave, and it is written as

$$\overrightarrow{E_i}=\overrightarrow{E_0}e^{j(k\cos\phi_0 x+k\sin\phi_0 y)}. \quad (3.11)$$

Eq. (3.10) can be written as

$$\overrightarrow{E_Z}=\overrightarrow{E_0}e^{jk(x\cos\phi_0+y\sin\phi_0)}+Ae^{-jk(x\cos\phi_0+y\sin\phi_0)}+Be^{-jk(x\cos\phi_0+y\sin\phi_0)}+Ce^{jk(x\cos\phi_0+y\sin\phi_0)}. \quad (3.12)$$

Eq. (3.12) is taken to derivative according to the parameter of y. It is shown as

$$\frac{d\overrightarrow{E_Z}}{dy}=jk\sin\phi_0\left[\overrightarrow{E_0}e^{jk(x\cos\phi_0+y\sin\phi_0)}-Ae^{-jk(x\cos\phi_0+y\sin\phi_0)}+Be^{-jk(x\cos\phi_0+y\sin\phi_0)}-Ce^{jk(x\cos\phi_0+y\sin\phi_0)}\right]. \quad (3.13)$$

Eq. (3.2) can be rewritten as

$$\overrightarrow{E_Z}|_{y=0}=\frac{Z}{j\omega\mu_0}\frac{d\overrightarrow{E_Z}}{dy}|_{y=0}. \quad (3.14)$$

We will substitute Eq. (3.12) and Eq. (3.13) instead of Eq. (3.14). So, the obtained equation can be written as

$$\left(\overrightarrow{E_0}+C\right)e^{jkx\cos\phi_0}+(A+B)e^{-jkx\cos\phi_0}=\frac{Zk\sin\phi_0}{\omega\mu_0}\left[\left(\overrightarrow{E_0}-C\right)e^{jkx\cos\phi_0}-(A-B)e^{-jkx\cos\phi_0}\right]. \quad (3.15)$$

Eq. (3.15) can be rearranged as

$$\overrightarrow{E_0} + C = \frac{kZ\sin\phi_0}{\omega\mu_0}\left(\overrightarrow{E_0} - C\right) \tag{3.16}$$

where Z is equal to $\left(\frac{Z_0}{\sin\theta}\right)$. Eq. (3.16) can be rewritten as

$$\sin\theta\overrightarrow{E_0} + \sin\theta C = \sin\phi_0\overrightarrow{E_0} - \sin\phi_0 C\,. \tag{3.17}$$

Eq. (3.17) can be rearranged as

$$C = \frac{\sin\phi_0 - \sin\theta}{\sin\phi_0 + \sin\theta}\overrightarrow{E_0} \tag{3.18}$$

where R, which is called as reflection coefficient of impedance surface, is equal to $\left[\frac{\sin\phi_0 - \sin\theta}{\sin\phi_0 + \sin\theta}\right]$, and C is defined as reflection coefficient separated from the surface. Consequently, the reflected electric and magnetic fields on the surface are obtained as

$$\overrightarrow{E_r} = \overrightarrow{e_Z}\overrightarrow{E_0}\,Re^{jk(x\cos\phi_0 - y\sin\phi_0)} \tag{3.19}$$

and,

$$\overrightarrow{H_r} = \overrightarrow{e_z}\frac{\overrightarrow{E_0}R}{Z}\left(\sin\phi_0\overrightarrow{e_x} + \cos\phi_0\overrightarrow{e_y}\right)e^{jk(x\cos\phi_0 - y\sin\phi_0)} \tag{3.20}$$

,respectively, and the incident electric and magnetic fields on the surface are obtained as

$$\overrightarrow{E_i} = \overrightarrow{e_Z}\overrightarrow{E_0}e^{jk(x\cos\phi_0 + y\sin\phi_0)} \tag{3.21}$$

and,

$$\overrightarrow{H_i} = -\frac{\overrightarrow{E_0}}{Z_0}\left(\sin\phi_0\overrightarrow{e_x} - \cos\phi_0\overrightarrow{e_y}\right)e^{jk(x\cos\phi_0 + y\sin\phi_0)} \tag{3.22}$$

,respectively, where Z_0, which is called as free space impedance, is equal to $\sqrt{\frac{\mu_0}{\varepsilon_0}}$ or $Z\sin\theta$. After finding the incident and reflected electric and magnetic fields, the electric and magnetic field densities coming to the impedance surface must be

found. The electric field density, $\overrightarrow{J_{es}}$, is equal to $\vec{n}\times\overrightarrow{H_T}|_S$ or $\overrightarrow{e_y}\times\overrightarrow{H_T}|_{y=0}$. Eq. (3.20) is inserted into the formula of $\overrightarrow{J_{es}}$. It is obtained as

$$\overrightarrow{J_{es}} = 2\frac{\sin\theta}{\sin\phi_0+\sin\theta}\vec{n}\times\overrightarrow{H_i}|_S \tag{3.23}$$

where the equation of $\left(2\vec{n}\times\overrightarrow{H_i}\right)$ defines as physical optics, and the expression of $\sin\theta\to\infty$ is defined as perfect electric surfaces. Otherwise, the magnetic field density, $\overrightarrow{J_{ms}}$, is equal to $\left(-\vec{n}\times\vec{E}|_S\right)$, where $\vec{E}$ is equal to $\left(\overrightarrow{E_i}+\overrightarrow{E_r}\right)$. The sum of Eqs. (3.19) and (3.21) are inserted into the formula of $\overrightarrow{J_{ms}}$. It is obtained as

$$\overrightarrow{J_{ms}} = -2\frac{\sin\phi_0}{\sin\phi_0+\sin\theta}\vec{n}\times\overrightarrow{E_i}|_S\,. \tag{3.24}$$

If we know the fields that come to the impedance surface, we can write the current densities. In this manner, both electric and magnetic current densities are obtained as

$$\vec{A} = \frac{\mu_0}{2\pi}\iint\frac{\sin\theta}{\sin\alpha+\sin\theta}\vec{n}\times\overrightarrow{H_i}|_S\,\frac{e^{-jkR}}{R}dS' \tag{3.25}$$

and,

$$\vec{F} = -\frac{\varepsilon_0}{2\pi}\iint\frac{\sin\alpha}{\sin\alpha+\sin\phi}\vec{n}\times\overrightarrow{E_i}|_S\,\frac{e^{-jkR}}{R}dS' \tag{3.26}$$

,respectively. ϕ_0 changes in cylindrical and spherical waves, so in the equations of current densities, we need to substitute α instead of ϕ_0.

After obtaining the electric field and magnetic field intensities, the expression of scattered field can be written as

$$\overrightarrow{E_S} = -J\omega\vec{A} - \frac{1}{\varepsilon_0}\nabla\times\vec{F}\,. \tag{3.27}$$

Eqs. (3.25) and (3.26) are inserted into Eq. (3.27), and so, Eq. (3.27) can be rewritten as

$$\overrightarrow{E_S} = -\frac{j\omega\mu_0}{2\pi}\iint \frac{\sin\theta}{\sin\alpha+\sin\theta}\vec{n}\times\overrightarrow{H_i}|_S \frac{e^{-jkR}}{R}dS' + \frac{1}{2\pi}\iint \frac{\sin\alpha}{\sin\alpha+\sin\theta}\nabla_P\times\left[\vec{n}\times\overrightarrow{E_i}|_S \frac{e^{-jkR}}{R}\right]dS' \qquad (3.28)$$

where ∇_P defines as the rotational, and the equation of $\nabla_P\times\left[\vec{n}\times\overrightarrow{E_i}|_S \frac{e^{-jkR}}{R}\right]$ is equal to $\overrightarrow{E_0}e^{jkx'\cos\phi_0}(-jk)\frac{e^{-jkR}}{R}\left[\overrightarrow{e_y}\frac{z-z'}{R}-\overrightarrow{e_z}\frac{y}{R}\right]$.

After obtaining the scattered expression, we need to calculate at the P observation point of all the rays coming to the x' point as shown in Fig. 5.

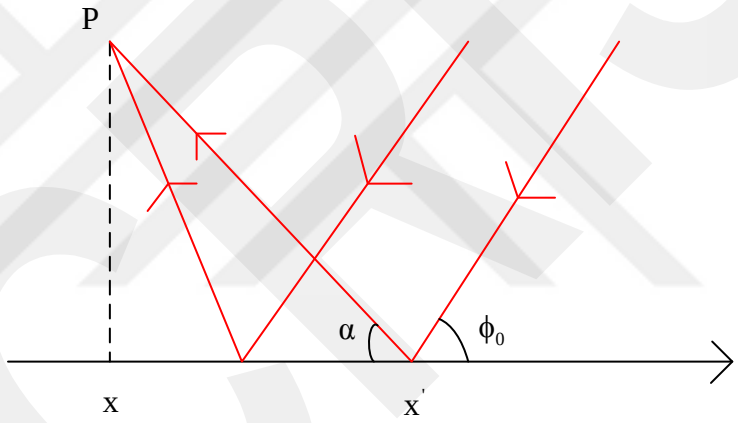

Fig. 5. Rays coming to the observation point P

Eq. (3.28) can be rewritten as

$$\overrightarrow{E_S} = \frac{J}{2\pi}\overrightarrow{\varepsilon_0}\iint\left[\left(\frac{-\sin\phi_0}{Z_0}\right)\left(\frac{\sin\theta\omega\mu_0}{\sin\alpha+\sin\theta}\right)\overrightarrow{e_z} + k\frac{y}{R}\frac{\sin\alpha}{\sin\alpha+\sin\theta}\overrightarrow{e_z} - k\frac{z-z'}{R}\frac{\sin\alpha}{\sin\alpha+\sin\theta}\overrightarrow{e_y}\right] \times e^{jkx'\cos\phi_0}\frac{e^{-jkR}}{R}dx'dz' \qquad (3.29)$$

where k, the wave number is equal to $\frac{\omega\mu_0}{Z_0}$. z' part of the integrand of Eq. (3.29) will be calculated. It is written as

$$g(z') = R - \left[(x-x')^2 + y^2 + (z-z')^2\right]^{1/2}. \qquad (3.30)$$

Eq. (3.30) is rearranged as

$$\frac{d\gamma}{dz'} = -\frac{z - z'}{R}. \tag{3.31}$$

When Eq. (3.31) is equal to zero, the stationary phase function, which is showed as $z_s = z$, is obtained. Since the amplitude term of the stationary phase function changes slowly, we only need to take the first term. The first term can be written as

$$f(x', z_s) = \frac{\sin\alpha \frac{y}{R_S} - \sin\phi_0 \sin\theta}{\sin\alpha + \sin\theta} \vec{e_z} \tag{3.32}$$

where x' is defined as the amplitude function. In this manner, the first two terms of Eq. (3.29) is combined and because of $z = z'$, its third term disappears. Eq. (3.30) can be rewritten as

$$g(z_s') = R_S + \frac{1}{2R_S}(z' - z)^2. \tag{3.33}$$

Eq. (3.29) can be rewritten as

$$\vec{E_S} = \vec{e_z} \frac{jk\vec{E_0}}{2\pi} \int_{x'=0}^{\infty} \frac{\sin\alpha \frac{y}{R_S} - \sin\phi_0 \sin\theta}{\sin\alpha + \sin\theta} e^{jkx'\cos\phi_0} \frac{e^{-jkR_S}}{R_S} \times \int_{-\infty}^{\infty} e^{-jk\frac{1}{2R_S}(z'-z)^2} dz' \tag{3.34}$$

The error function can be applied in the expression of $\int_{-\infty}^{\infty} e^{-jk\frac{1}{2R_S}(z'-z)^2} dz'$ in Eq. (3.34). The error function is defined as

$$\int_{-\infty}^{\infty} e^{\frac{y^2}{2}} dy = \sqrt{2\pi}. \tag{3.35}$$

Eq. (3.35) is inserted into Eq. (3.34). As a result, the scattered electric field [2] is obtained as

$$\overrightarrow{E_S} = \overrightarrow{e_z} \frac{k e^{j\frac{\pi}{4}} \overrightarrow{E_0}}{\sqrt{2\pi}} \int_{x'=0}^{\infty} \frac{\frac{y}{R_S}\sin\alpha - \sin\phi_0 \sin\theta}{\sin\alpha + \sin\theta} e^{jkx'\cos\phi_0} \frac{e^{-jkR_S}}{\sqrt{kR_S}} dx' \qquad (3.36)$$

where R_S is equal to $\sqrt{\left[(x-x')^2 + y^2\right]}$.

3.2. THE INCIDENT AND REFLECTED PO EQUATIONS

From the obtaining scattered electric field equation in Eq.(3.36), both the incident and reflected PO equations in the half plane are obtained. Since the integrand of Eq. (3.36) goes infinity, we cannot apply the method of far field approximation to Eq. (3.36). Therefore, The Stationary phase method was applied to this above integral. With this method, the discontinuous point was taken out and the continuous points were calculated. Because this method gives points that are continuous on the surface. If this method is applied, this area should be limited to U(x).

At the $x^{'}$ point, the radiation goes at an angle. It is shown in the Fig. 6.

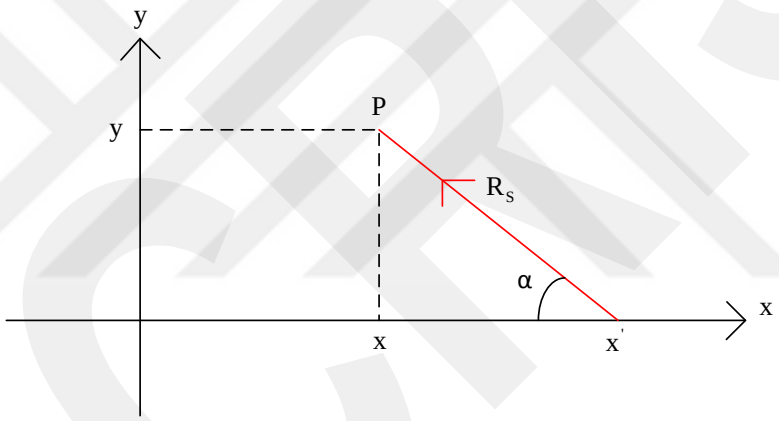

Fig. 6. Angular propagation of the radiation at the $x^{'}$ point

The integrand of $\overrightarrow{E_S}$ is both multiplied and divided by $(\cos\phi_0 - \cos\beta)$. Eq. (3.36) can be rewritten as

$$\overrightarrow{E_S} = \overrightarrow{e_z}\frac{ke^{j\frac{\pi}{4}}\overrightarrow{E_0}}{\sqrt{2\pi}}\int_{x'=0}^{\infty}\left(\frac{\cos\phi_0-\cos\beta}{\cos\phi_0-\cos\beta}\right)\left[\frac{\frac{y}{R_S}\sin\alpha-\sin\phi_0\sin\theta}{\sin\alpha+\sin\theta}\right]e^{jkx'\cos\phi_0} \times\frac{e^{-jkR_S}}{\sqrt{kR_S}}dx' \quad . \quad (3.37)$$

The trigonometric relations of

$$\frac{1}{\cos\phi_0-\cos\beta}=\frac{1}{2\sin\phi_0}\left[\cot g\frac{\beta-\phi_0}{2}-\cot g\frac{\beta+\phi_0}{2}\right] \tag{3.38}$$

can be obtained for soft surfaces [1]. Eq. (3.37) is rearranged as

$$\overrightarrow{E_S}=\overrightarrow{e_z}\frac{ke^{j\frac{\pi}{4}}\overrightarrow{E_0}}{\sqrt{2\pi}}\int_{x'=0}^{\infty}\left(\frac{1}{\cos\phi_0-\cos\beta}\right)\left[\frac{\frac{y}{R_S}\sin\alpha-\sin\phi_0\sin\theta}{\sin\alpha+\sin\theta}\right](\cos\phi_0-\cos\beta)\cdot \tag{3.39}$$
$$\times e^{jkx'\cos\phi_0}\frac{e^{-jkR_S}}{\sqrt{kR_S}}dx'$$

Eq. (3.38) is inserted into Eq. (3.39). It is written as

$$\overrightarrow{E_S}=\overrightarrow{e_z}\frac{ke^{j\frac{\pi}{4}}\overrightarrow{E_0}}{\sqrt{2\pi}}\int_{x'=0}^{\infty}\frac{1}{2\sin\phi_0}\left[\cot g\frac{\beta-\phi_0}{2}-\cot g\frac{\beta+\phi_0}{2}\right]\left[\frac{\frac{y}{R_S}\sin\alpha-\sin\phi_0\sin\theta}{\sin\alpha+\sin\theta}\right]. \tag{3.40}$$
$$\times(\cos\phi_0-\cos\beta)e^{jkx'\cos\phi_0}\frac{e^{-jkR_S}}{\sqrt{kR_S}}dx'$$

Eq.(3.40) is rearranged as

$$\overrightarrow{E_S}=\overrightarrow{e_z}\frac{ke^{j\frac{\pi}{4}}\overrightarrow{E_0}}{2\sqrt{2\pi}\sin\phi_0}\int_{x'=0}^{\infty}\left[\cot g\frac{\beta-\phi_0}{2}-\cot g\frac{\beta+\phi_0}{2}\right]\left[\frac{\frac{y}{R_S}\sin\alpha-\sin\phi_0\sin\theta}{\sin\alpha+\sin\theta}\right]. \tag{3.41}$$
$$\times(\cos\phi_0-\cos\beta)e^{jkx'\cos\phi_0}\frac{e^{-jkR}}{\sqrt{kR_S}}dx'$$

In this manner, based on the Eq. (3.41), the PO integrals may be explained as

$$\overrightarrow{E_{PO_1}}(P)=\overrightarrow{e_z}\frac{ke^{j\frac{\pi}{4}}\overrightarrow{E_0}}{2\sqrt{2\pi}}\int_{x'=0}^{\infty}\left[\cot g\frac{\beta-\phi_0}{2}\right]\left[\frac{\frac{y}{R_S}\sin\alpha-\sin\phi_0\sin\theta}{\sin\alpha+\sin\theta}\right]\left(\frac{\cos\phi_0-\cos\beta}{\sin\phi_0}\right) \tag{3.42}$$
$$\times e^{jkx'\cos\phi_0}\frac{e^{-jkR_S}}{\sqrt{kR_S}}dx'$$

and

$$\overrightarrow{E_{PO_2}}(P) = -\vec{e}_z \frac{ke^{j\frac{\pi}{4}}\overrightarrow{E_0}}{2\sqrt{2\pi}} \int_{x'=0}^{\infty} \left[\cot g \frac{\beta+\phi_0}{2}\right] \left[\frac{\frac{y}{R_S}\sin\alpha - \sin\phi_0 \sin\theta}{\sin\alpha + \sin\theta}\right] \left(\frac{\cos\phi_0 - \cos\beta}{\sin\phi_0}\right) \quad (3.43)$$

$$\times e^{jkx'\cos\phi_0} \frac{e^{-jkR_S}}{\sqrt{kR_S}} dx'$$

where R_S is equal to $\sqrt{\left[(x-x')^2 + y^2\right]}$ for both soft and hard surfaces, respectively [1]. The soft surface is emphasized on this thesis. Thus, we will use Eq. (3.42). According Ref [1], The cotangent functions in the integrand of Eqs. (3.42) and (3.43) can be written as

$$\cot g \frac{\beta \mp \phi_0}{2} = \tan \frac{\pi - (\beta \mp \phi_0)}{2}. \quad (3.44)$$

Because the soft surface is emphasized on this thesis, the cotangent function in the integrand of Eq. (3.42), which is equal to $\cot g \frac{\beta - \phi_0}{2} = \tan \frac{\pi - (\beta - \phi_0)}{2}$, will be used.

The geometry of wedge diffraction [1], which is shown in Fig. 7, will be considered.

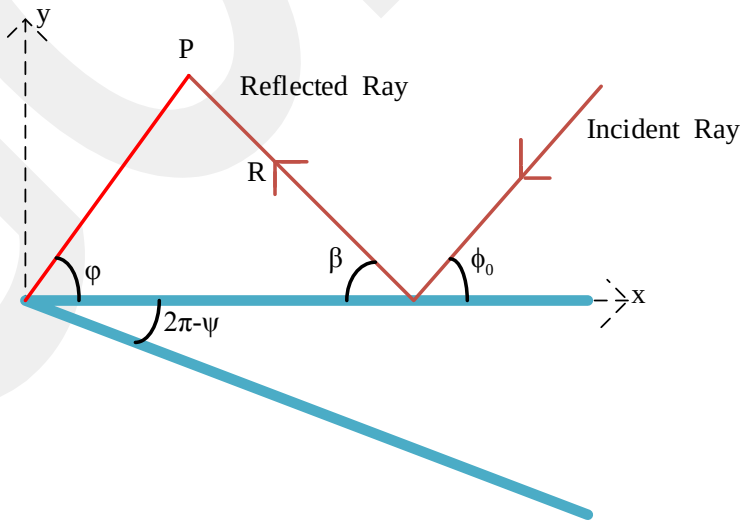

Fig. 7. Diffraction geometry of the wedge

According to Fig. 7, the outer angle of the wedge, which is shown as ψ, is equal to $n\pi$, where n is the parameter. Since the outer angle of half-plane is

equal to 2π, n is equal to 2 for half-plane. Based on this information, Eq. (3.44) can be written as

$$\cot g\frac{\beta\mp\phi_0}{2}=\sin\left(\pi/n\right)\frac{\cos\left(\pi/n\right)-\sin\left\{\frac{\left[\pi-\left(\beta\mp\phi_0\right)\right]}{n}\right\}}{\cos\left(\pi/n\right)-\cos\left\{\frac{\left[\pi-\left(\beta\mp\phi_0\right)\right]}{n}\right\}}|_{n=2} \tag{3.45}$$

for wedge diffraction [1]. Because the soft surface is emphasized on this thesis, the cotangent function in the integrand of Eq. (3.45), which is equal to $\left\{\cot g\frac{\beta-\phi_0}{2}=\sin\left(\pi/n\right)\frac{\cos\left(\pi/n\right)-\sin\left\{\frac{\pi-\left(\beta-\phi_0\right)}{n}\right\}}{\cos\left(\pi/n\right)-\cos\left\{\frac{\pi-\left(\beta-\phi_0\right)}{n}\right\}}|_{n=2}\right\}$, will be used. So, the cotangent function in the integrand of Eq. (3.45) for soft surface is inserted into Eq. (3.42). In this manner, the PO integrals for soft surface can be expressed as

$$\overrightarrow{E_{PO_1}}(P)=\overrightarrow{e_z}\frac{ke^{j\frac{\pi}{4}}\overrightarrow{E_0}}{2\sqrt{2\pi}}\int_{x'=0}^{\infty}\left[\sin\left(\pi/n\right)\frac{\cos\left(\pi/n\right)-\sin\left\{\frac{\pi-\left(\beta-\phi_0\right)}{n}\right\}}{\cos\left(\pi/n\right)-\cos\left\{\frac{\pi-\left(\beta-\phi_0\right)}{n}\right\}}|_{n=2}\right]\left(\frac{\cos\phi_0-\cos\beta}{\sin\phi_0}\right) \tag{3.46}$$
$$\times e^{jkx'\cos\phi_0}\frac{e^{-jkR_S}}{\sqrt{kR_S}}dx'$$

and

$$\overrightarrow{E_{PO_2}}(P)=-\overrightarrow{e_z}\frac{ke^{j\frac{\pi}{4}}\overrightarrow{E_0}}{2\sqrt{2\pi}}\int_{x'=0}^{\infty}\left[\sin\left(\pi/n\right)\frac{\cos\left(\pi/n\right)-\sin\left\{\frac{\pi-\left(\beta-\phi_0\right)}{n}\right\}}{\cos\left(\pi/n\right)-\cos\left\{\frac{\pi-\left(\beta-\phi_0\right)}{n}\right\}}|_{n=2}\right]\left(\frac{\cos\phi_0-\cos\beta}{\sin\phi_0}\right) \tag{3.47}$$
$$\times e^{jkx'\cos\phi_0}\frac{e^{-jkR_S}}{\sqrt{kR_S}}dx'$$

for the parts of reflected and incident, respectively. Because Eqs. (3.46) and (3.47) are obtained, the total PO integral for soft surface, $\overrightarrow{E_{PO_{(Soft)}}}$, which is equal to $\left(\overrightarrow{E_{PO_1}}+\overrightarrow{E_{PO_2}}\right)$, can be written.

The coefficient of the cotangent function for soft surface in the integrands of Eqs. (3.46) and (3.47) will be multiplied by the expression of $\left[\frac{\mp 1}{\cos\left(\pi/n\right)-\sin\left(\pi/n\right)}\right]$, respectively. The goal is to eliminate this coefficient and it must be the value of 1 in the stational phase method. In this manner, Eqs. (3.46) and (3.47) can be rewritten as

$$\overrightarrow{U_{PO_1}}(P)=\vec{e}_z\frac{ke^{j\frac{\pi}{4}}\overrightarrow{E_0}}{2\sqrt{2\pi}}\int_{x'=0}^{\infty}\left[\frac{\frac{y}{R_S}\sin\alpha-\sin\phi_0\sin\theta}{\sin\alpha+\sin\theta}\right]\left[\sin\left(\pi/n\right)\frac{\cos\left(\pi/n\right)-\sin\left\{\frac{\pi-(\beta-\phi_0)}{n}\right\}}{\cos\left(\pi/n\right)-\cos\left\{\frac{\pi-(\beta-\phi_0)}{n}\right\}}\right] \tag{3.48}$$

$$\times\left[\frac{-1}{\cos\left(\pi/n\right)-\sin\left(\pi/n\right)}\right]\left(\frac{\cos\phi_0-\cos\beta}{\sin\phi_0}\right)e^{jkx'\cos\phi_0}\frac{e^{-jkR_S}}{\sqrt{kR_S}}dx'$$

and

$$\overrightarrow{U_{PO_2}}(P)=-\vec{e}_z\frac{ke^{j\frac{\pi}{4}}\overrightarrow{E_0}}{2\sqrt{2\pi}}\int_{x'=0}^{\infty}\left[\frac{\frac{y}{R_S}\sin\alpha-\sin\phi_0\sin\theta}{\sin\alpha+\sin\theta}\right]\left[\sin\left(\pi/n\right)\frac{\cos\left(\pi/n\right)-\sin\left\{\frac{\pi-(\beta-\phi_0)}{n}\right\}}{\cos\left(\pi/n\right)-\cos\left\{\frac{\pi-(\beta-\phi_0)}{n}\right\}}\right] \tag{3.49}$$

$$\times\left[\frac{1}{\cos\left(\pi/n\right)-\sin\left(\pi/n\right)}\right]\left(\frac{\cos\phi_0-\cos\beta}{\sin\phi_0}\right)e^{jkx'\cos\phi_0}\frac{e^{-jkR}}{\sqrt{kR_S}}dx'$$

where R_S is equal to $\sqrt{\left[(x-x')^2+y^2\right]}$, respectively. Eqs. (3.48) and (3.49) can be expressed as the parts of both reflected and incident for half-plane to wedge.

In order to obtain the PO integrals in half-plane, we need to apply the stational phase method in the parts of both reflected and incident the integral. Therefore, the coefficient of $\left[\frac{\frac{y}{R_S}\sin\alpha-\sin\phi_0\sin\theta}{\sin\alpha+\sin\theta}\right]$ is neglected to obtain the PO integrals in half-plane. In addition, the stational phase method tells us what its contribution is to the radiation at continuous points. Thus, the equation of R_S must be differentiated with respect to x'. When the stational phase method is applied, the expression can be obtained as

$$p\left(x^{'}\right) = x^{'}\cos\phi_0 - R_S . \tag{3.50}$$

When Eq. (3.50) is differentiated with respect to $x^{'}$, Eq. (3.50) can be rewritten as

$$\frac{dP}{dx^{'}} = \cos\phi_0 - \left(\frac{x - x^{'}}{R_S}\right). \tag{3.51}$$

Eq.(3.51) is needed to use the phase function. According to Fig. 2, Eq. (3.51) can be rewritten as

$$\frac{dP}{dx^{'}} = \cos\phi_0 - \cos\alpha . \tag{3.52}$$

To be able to apply the stational phase method, Eq.(3.52) is equal to zero. In this manner, two phase points are obtained as $\alpha_{S_1} = \phi_0$ and $\alpha_{S_2} = -\phi_0$. These phase points are shown in Fig. 8 and Fig. 9, respectively.

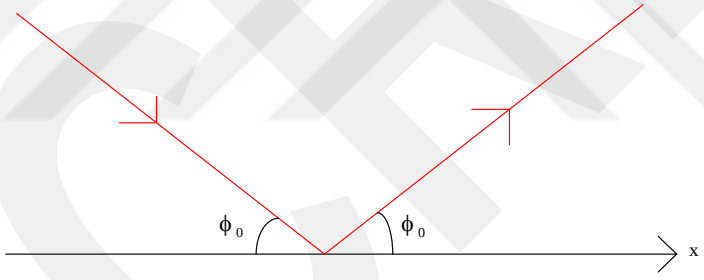

Fig. 8. First stational phase point, $\alpha_{S_1} = \phi_0$

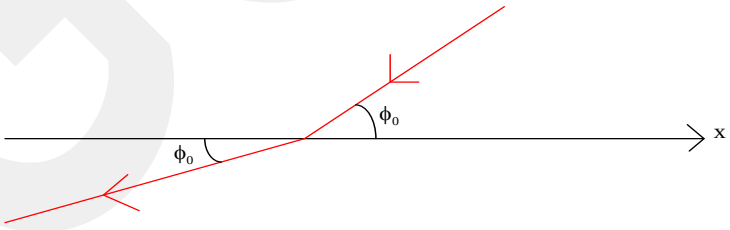

Fig. 9. Second stational phase point, $\alpha_{S_2} = -\phi_0$

Eq. (3.52) is differentiated with respect to $x^{'}$. Eq. (3.52) can be rewritten as

$$\frac{d^2P}{dx^{'2}} = \sin\alpha \frac{d\alpha}{dx^{'}} \tag{3.53}$$

where $\sin\alpha$ is equal to $\left(\frac{y}{R_S}\right)$. Because the stational phase point is calculated according to α in Fig. 8 and Fig. 9, the expression with term α is derived with respect to $x^{'}$ in Eq. (3.53). Thus, the stational phase value of R_S, which is defined as R_{S_1}, is equal to $\left(\sqrt{(x-x_S)^2+y^2}\right)$, where x_S is equal to $\mp\phi_0$ shown in Fig. 10.

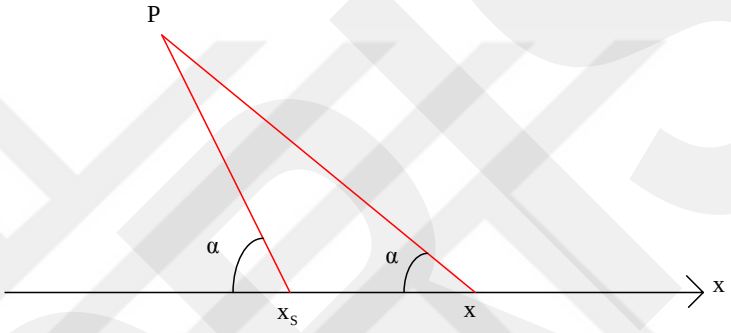

Fig. 10. The stational phase point, $x_S = \mp\phi_0$

Now, we take into account the reflected part in order to calculate the first stational phase point, which is defined as $\alpha_{S_1} = \phi_0$. In the first stational phase point, $x^{'}$ is defined as x_s, R_S is defined as R_{S_1}, and β is defined as ϕ_0. Thus, Eq. (3.48) can be rearranged as

$$\overrightarrow{E_{PO_1}}(P) = \vec{e}_z \frac{ke^{j\frac{\pi}{4}}\overrightarrow{E_0}}{2\sqrt{2\pi}} \left[\sin\left(\pi/n\right) \frac{\cos\left(\pi/n\right) - \sin\left\{\frac{\pi-(\beta-\phi_0)}{n}\right\}}{\cos\left(\pi/n\right) - \cos\left\{\frac{\pi-(\beta-\phi_0)}{n}\right\}} \right] \left(\frac{-1}{\cos\left(\pi/n\right) - \sin\left(\pi/n\right)} \right) . \tag{3.54}$$
$$\times \left(\frac{\cos\phi_0 - \cos\beta}{\sin\phi_0} \right) \frac{1}{\sqrt{kR_{S_1}}} e^{jk\left(x_s\cos\phi_0 - R_{S_1}\right)} \int_{-\infty}^{\infty} e^{-jk\frac{\sin^2\phi_0}{2R_{S_1}}(x-x_s)^2} dx_s U(-\xi)$$

Eq. (3.54) can be rearranged as

$$\overrightarrow{E_{PO_1}}(P)=\overrightarrow{e_z}\frac{ke^{j\frac{\pi}{4}}\overrightarrow{E_0}}{2\sqrt{2\pi}}\left[\sin\left(\pi/n\right)\left\{\cos\left(\pi/n\right)-\sin\left(\frac{\pi-(\beta-\phi_0)}{n}\right)\right\}\right]\frac{1}{\sqrt{kR_{S_1}}}e^{jk\left(x_s\cos\phi_0-R_{S_1}\right)}$$
$$\times\frac{(\cos\phi_0-\cos\beta)}{\sin\phi_0\left\{\cos\left(\pi/n\right)-\cos\left(\frac{\pi-(\beta-\phi_0)}{n}\right)\right\}}\int_{-\infty}^{\infty}e^{-jk\frac{\sin^2\phi_0}{2R_{S_1}}\left(x'-x_s\right)^2}dx_sU(-\xi) \quad . \quad (3.55)$$

According to the parameter of β, The L'Hopital's Rule can be applied in Eq. (3.55). Thus, Eq. (3.55) can be rewritten as

$$\overrightarrow{E_{PO_1}}(P)=\overrightarrow{e_z}\frac{ke^{j\frac{\pi}{4}}\overrightarrow{E_0}}{2\sqrt{2\pi}}\left[\sin\left(\pi/n\right)\left\{\cos\left(\pi/n\right)-\sin\left(\frac{\pi-(\beta-\phi_0)}{n}\right)\right\}\right]\frac{1}{\sqrt{kR_{S_1}}}e^{jk\left(x_s\cos\phi_0-R_{S_1}\right)}$$
$$\times\left[\lim_{\beta\to\phi_0}\left(\frac{\cos\phi_0-\cos\beta}{\sin\phi_0\left[\cos\left(\pi/n\right)-\cos\left\{\frac{\pi-(\beta-\phi_0)}{n}\right\}\right]}\right)\right]\int_{-\infty}^{\infty}e^{-jk\frac{\sin^2\phi_0}{2R_{S_1}}(x-x_s)^2}dx_sU(-\xi) \quad . \quad (3.56)$$

If The L'Hopital's Rule is applied in Eq. (3.56), Eq. (3.56) can be rewritten as

$$\overrightarrow{E_{PO_1}}(P)=\overrightarrow{e_z}\frac{ke^{j\frac{\pi}{4}}\overrightarrow{E_0}}{2\sqrt{2\pi}}\left[\sin\left(\pi/n\right)\left\{\cos\left(\pi/n\right)-\sin\left(\frac{\pi-(\beta-\phi_0)}{n}\right)\right\}\right]\frac{1}{\sqrt{kR_{S_1}}}e^{jk\left(x_s\cos\phi_0-R_{S_1}\right)}$$
$$\times\left[\lim_{\beta\to\phi_0}\frac{\sin\beta}{\left(-1/n\right)\sin\left\{\frac{\pi-(\beta-\phi_0)}{n}\right\}}\right]\int_{-\infty}^{\infty}e^{-jk\frac{\sin^2\phi_0}{2R_{S_1}}(x-x_s)^2}dx_sU(-\xi) \quad . \quad (3.57)$$

After applying The L'Hopital's Rule in Eq. (3.57), Eq. (3.57) can be expressed as

$$\overrightarrow{E_{PO_1}}(P)=\overrightarrow{e_z}\frac{ke^{j\frac{\pi}{4}}\overrightarrow{E_0}}{2\sqrt{2\pi}}\left[\sin\left(\pi/n\right)\left\{\cos\left(\pi/n\right)-\sin\left(\frac{\pi-(\beta-\phi_0)}{n}\right)\right\}\right]\frac{1}{\sqrt{kR_{S_1}}}e^{jk\left(x_s\cos\phi_0-R_{S_1}\right)}$$
$$\times\left\{\frac{\sin\phi_0}{\left(-1/n\right)\sin\left(\pi/n\right)}\right\}\int_{-\infty}^{\infty}e^{-jk\frac{\sin^2\phi_0}{2R_{S_1}}(x-x_s)^2}dx_sU(-\xi) \quad (3.58)$$

The conversion in Ref. [2] can be written as

$$-jk\frac{\sin^2\phi_0}{2R_{S_1}}\left(x'-x_s\right)^2=-\frac{y^2}{2}. \quad (3.59)$$

Because y is equal to $\left(\frac{x}{\sin\phi_0}\right)$ according to Fig. 6, Eq. (3.59) can be rearranged as

$$x - x' = e^{-j\frac{\pi}{4}}\sqrt{\frac{R_{S_1}}{k}}y. \tag{3.60}$$

When Eq. (3.60) is derived with respect to x', Eq. (3.60) can be rewritten as

$$dx' = e^{-j\frac{\pi}{4}}\sqrt{\frac{R_{S_1}}{k}}\frac{1}{\sin\phi_0}dy. \tag{3.61}$$

Eqs. (3.59) and (3.61) is inserted into Eq. (3.58). So, Eq. (3.58) can be rewritten as

$$\overrightarrow{E_{PO_1}}(P) = \overrightarrow{e_z}\frac{ke^{j\frac{\pi}{4}}\overrightarrow{E_0}}{2\sqrt{2\pi}}\left[\sin\left(\pi/n\right)\left\{\cos\left(\pi/n\right) - \sin\left(\frac{\pi-(\beta-\phi_0)}{n}\right)\right\}\right]\frac{1}{\sqrt{kR_{S_1}}}e^{jk\left(x_s\cos\phi_0 - R_{S_1}\right)} \times\left[\frac{\sin\phi_0}{\left(-1/n\right)\sin\left(\pi/n\right)}\right]\int_{-\infty}^{\infty}e^{-y^2/2}e^{-j\frac{\pi}{4}}\sqrt{\frac{R_{S_1}}{k}}\frac{1}{\sin\phi_0}dyU(-\xi) \tag{3.62}$$

When simplifying the Eq. (3.62), Eq. (3.62) can be rearranged as

$$\overrightarrow{E_{PO_1}}(P) = \overrightarrow{e_z}\frac{e^{j\frac{\pi}{4}}\overrightarrow{E_0}}{2\sqrt{2\pi}}\left[\cos\left(\pi/n\right) - \sin\left\{\frac{\pi-(\beta-\phi_0)}{n}\right\}\right]e^{jk\left(x_s\cos\phi_0 - R_{S_1}\right)} \times\frac{1}{\left(-1/n\right)}e^{-j\frac{\pi}{4}}\int_{-\infty}^{\infty}e^{-y^2/2}dyU(-\xi) \tag{3.63}$$

Eq. (3.35), which is defined as the error function, is inserted into Eq. (3.63). Eq. (3.63) can be rewritten as

$$\overrightarrow{E_{PO_1}}(P) = \overrightarrow{e_z}\frac{\overrightarrow{E_0}}{2}\left[\frac{n\cos\left(\pi/n\right) - \sin\left\{\frac{\pi-(\beta-\phi_0)}{n}\right\}}{\cos\left(\pi/n\right) - \sin\left(\pi/n\right)}\right]e^{jk\left(x_S\cos\phi_0 - R_{S_1}\right)}U(-\xi). \tag{3.64}$$

If we remember, it is clear that n is equal to 2 for a half-plane from because the outer angle of a half-plane is 2π [1]. Thus, Eq. (3.64) can be rewritten as

$$\overrightarrow{E_{PO_1}}(P)=\overrightarrow{e_z}\frac{\overrightarrow{E_0}}{2}\left[\frac{n\cos\left(\pi/n\right)-\sin\left\{\frac{\pi-(\beta-\phi_0)}{n}\right\}}{\cos\left(\pi/n\right)-\sin\left(\pi/n\right)}\Big|_{n=2}\right]e^{jk\left(x_S\cos\phi_0-R_{S_1}\right)}U(-\xi). \quad (3.65)$$

When Eq. (3.65) is rearranged, it is rewritten as

$$\overrightarrow{E_{PO_1}}(P)=\overrightarrow{e_z}\overrightarrow{E_0}e^{jk\left(x_S\cos\phi_0-R_{S_1}\right)}U(-\xi) \quad (3.66)$$

where R_{S_1} is equal to $\left[(x_s-x)\cos\phi_0+y\sin\phi_0\right]$ according to Fig. 11.

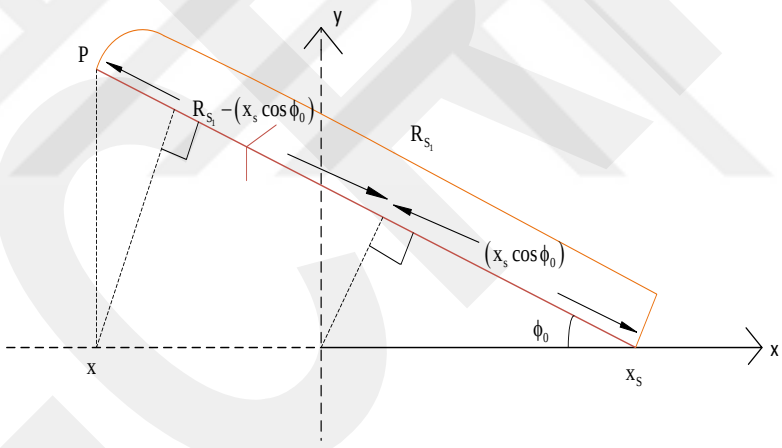

Fig. 11. The geometry of the reflection part

According to Fig. 11, the equation of R_{S_1} is attached in Eq. (3.66). Hence, Eq. (3.66) can be rewritten as

$$\overrightarrow{E_{PO_1}}(P)=\overrightarrow{e_z}\overrightarrow{E_0}e^{jk\left(x\cos\phi_0-y\sin\phi_0\right)}U(-\xi). \quad (3.67)$$

The term of ξ can be represented as

$$\xi=\mp\sqrt{k\left[g(x_e)-g(x_s)\right]} \quad (3.68)$$

which is the detour parameter, where $g(x_e)$ is equal to l_d, and $g(x_s)$ is equal to l_{GO} [2]. It is shown in Fig. 12.

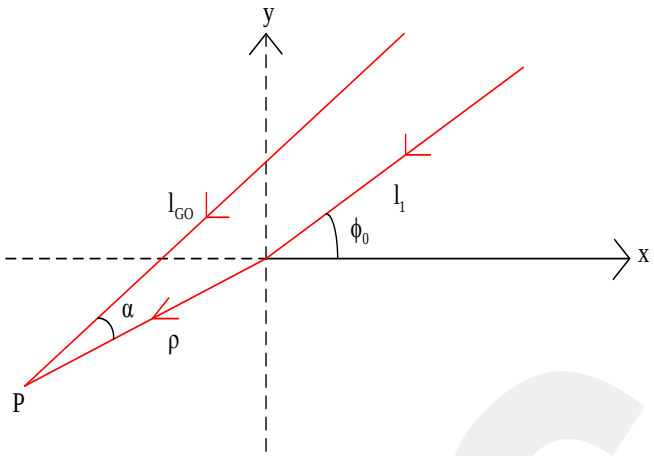

Fig. 12. The geometry of obtaining the detour parameter, ξ , for reflected part

Let $g(x_e)$ is l_d, and $g(x_S)$ is l_{GO}, according to Fig. 8, l_d is equal to $(\rho + l_1)$, l_{GO} is equal to $(l_1 + x)$, and x is equal to $(\rho\cos\alpha)$, where α is equal to $[\pi - (\phi - \phi_0)]$ according to Fig. 12.

Eq. (3.68) can be rearranged as

$$\xi = -\sqrt{k[l_d - l_{GO}]} \tag{3.69}$$

where $[l_d - l_{GO}]$ is equal to $\left[2\rho\cos^2\left(\frac{\phi - \phi_0}{2}\right)\right]$. Hence, Eq. (3.69) can be rewritten as

$$\xi = -\sqrt{2\rho k}\cos\left(\frac{\phi - \phi_0}{2}\right). \tag{3.70}$$

Eq.(3.70) is inserted into Eq.(3.67). As a result, the equation of the reflected part of PO equations can be obtained as

$$\overrightarrow{E_{PO_1}}(P) = \overrightarrow{e_z}\overrightarrow{E_0}e^{jk(x\cos\phi_0 - y\sin\phi_0)}U\left(\sqrt{2\rho k}\cos\left(\frac{\phi - \phi_0}{2}\right)\right). \tag{3.71}$$

Similarly, we take into account the incident part in order to calculate the second stational phase point, which is defined as $\alpha_{S_2} = -\phi_0$. In the second

stational phase point, x' is defined as x_s, R_S is defined as R_{S_1}, and β is defined as $-\phi_0$. Thus, Eq. (3.49) can be rearranged as

$$\overrightarrow{E_{PO_2}}(P) = -\vec{e}_z \frac{ke^{j\frac{\pi}{4}}\overrightarrow{E_0}}{2\sqrt{2\pi}} \int_{x'=0}^{\infty} \left[\sin\left(\pi/n\right) \frac{\cos\left(\pi/n\right) - \sin\left\{\frac{\pi-(\beta-\phi_0)}{n}\right\}}{\cos\left(\pi/n\right) - \cos\left\{\frac{\pi-(\beta-\phi_0)}{n}\right\}} \right] \times \left[\frac{1}{\cos\left(\pi/n\right) - \sin\left(\pi/n\right)} \right] \left(\frac{\cos\phi_0 - \cos\beta}{\sin\phi_0} \right) e^{jkx'\cos\phi_0} \frac{e^{-jkR_{S_1}}}{\sqrt{kR_{S_1}}} dx_s \quad . \quad (3.72)$$

Eq. (3.72) can be rearranged as

$$\overrightarrow{E_{PO_2}}(P) = -\vec{e}_z \frac{ke^{j\frac{\pi}{4}}\overrightarrow{E_0}}{2\sqrt{2\pi}} \left[\sin\left(\pi/n\right) \left\{ \cos\left(\pi/n\right) - \sin\left\{\frac{\pi-(\beta+\phi_0)}{n}\right\} \right\} \right] \frac{1}{\sqrt{kR_{S_1}}} e^{jk\left(x'\cos\phi_0 - R_{S_1}\right)} \times \left\{ \frac{(\cos\phi_0 - \cos\beta)}{\sin\phi_0 \left[\cos\left(\pi/n\right) - \cos\left\{\frac{\pi-(\beta+\phi_0)}{n}\right\} \right]} \right\} \int_{-\infty}^{\infty} e^{-jk\frac{\sin^2\phi_0}{R_{S_1}}\left(x'-x_s\right)^2} dx_s U(-\xi) \quad . \quad (3.73)$$

According to the parameter of β, The L'Hopital's Rule can be applied in Eq. (3.73). Thus, Eq. (3.73) can be rewritten as

$$\overrightarrow{E_{PO_2}}(P) = -\vec{e}_z \frac{ke^{j\frac{\pi}{4}}\overrightarrow{E_0}}{2\sqrt{2\pi}} \left[\sin\left(\pi/n\right) \left\{ \cos\left(\pi/n\right) - \sin\left\{\frac{\pi-(\beta+\phi_0)}{n}\right\} \right\} \right] \frac{1}{\sqrt{kR_{S_1}}} e^{jk\left(x'\cos\phi_0 - R_{S_1}\right)} \times \left[\lim_{\beta\to-\phi_0} \left\{ \frac{\cos\phi_0 - \cos\beta}{\sin\phi_0 \left(\cos\left(\pi/n\right) - \cos\left\{\frac{\pi-(\beta+\phi_0)}{n}\right\} \right)} \right\} \right] \int_{-\infty}^{\infty} e^{-jk\frac{\sin^2\phi_0}{2R_{S_1}}\left(x'-x_s\right)^2} dx_s U(-\xi) \quad . \quad (3.74)$$

If The L'Hopital's Rule is applied in Eq. (3.74), Eq. (3.74) can be rewritten as

$$\overrightarrow{E_{PO_2}}(P) = -\vec{e}_z \frac{ke^{j\frac{\pi}{4}}\overrightarrow{E_0}}{2\sqrt{2\pi}} \left[\sin\left(\pi/n\right) \left\{ \cos\left(\pi/n\right) - \sin\left\{\frac{\pi-(\beta+\phi_0)}{n}\right\} \right\} \right] \frac{1}{\sqrt{kR_{S_1}}} e^{jk\left(x'\cos\phi_0 - R_{S_1}\right)} \times \left[\lim_{\beta\to-\phi_0} \frac{-\sin\beta}{\left(-1/n\right)\sin\left\{\frac{\pi-(\beta+\phi_0)}{n}\right\}} \right] \int_{-\infty}^{\infty} e^{-jk\frac{\sin^2\phi_0}{2R_{S_1}}\left(x'-x_s\right)^2} dx_s U(-\xi) \quad . \quad (3.75)$$

After applying The L'Hopital's Rule in Eq. (3.75), Eq. (3.75) can be expressed as

$$\overrightarrow{E_{PO_2}}(P) = -\overrightarrow{e_z}\frac{ke^{j\frac{\pi}{4}}\overrightarrow{E_0}}{2\sqrt{2\pi}}\left[\sin\left(\pi/n\right)\left\{\cos\left(\pi/n\right)-\sin\left\{\frac{\pi-(\beta+\phi_0)}{n}\right\}\right\}\right]\frac{1}{\sqrt{kR_{S_1}}}e^{jk\left(x_s\cos\phi_0-R_{S_1}\right)} \quad . \quad (3.76)$$
$$\times\left[\frac{-\sin(-\phi_0)}{(-1/n)\sin\left(\pi/n\right)}\right]\int_{-\infty}^{\infty}e^{-jk\frac{\sin^2\phi_0}{2R_{S_1}}(x-x_s)^2}dx_sU(-\xi)$$

Eqs. (3.59), (3.60), and (3.61) are inserted into Eq. (3.76) [2]. Hereby, Eq. (3.76) can be rewritten as

$$\overrightarrow{E_{PO_2}}(P) = -\overrightarrow{e_z}\frac{ke^{j\frac{\pi}{4}}\overrightarrow{E_0}}{2\sqrt{2\pi}}\left[\sin\left(\pi/n\right)\left\{\cos\left(\pi/n\right)-\sin\left\{\frac{\pi-(\beta+\phi_0)}{n}\right\}\right\}\right]\frac{1}{\sqrt{kR_{S_1}}}e^{jk\left(x_s\cos\phi_0-R_{S_1}\right)} \quad . \quad (3.77)$$
$$\times\left[\frac{n\sin(-\phi_0)}{\sin\left(\pi/n\right)}\right]\int_{-\infty}^{\infty}e^{-y^2/2}e^{-j\frac{\pi}{4}}\sqrt{\frac{R_{S_1}}{k}}\frac{1}{\sin\phi_0}dyU(-\xi)$$

When simplifying the Eq. (3.77), Eq. (3.77) can be rearranged as

$$\overrightarrow{E_{PO_2}}(P) = -\overrightarrow{e_z}\frac{\overrightarrow{E_0}}{2\sqrt{2\pi}}\left[\frac{\cos\left(\pi/n\right)-\sin\left\{\frac{\pi-(\beta+\phi_0)}{n}\right\}}{\cos\left(\pi/n\right)-\sin\left(\pi/n\right)}\right]e^{jk\left(x_s\cos\phi_0-R_{S_1}\right)}\left[\frac{n\sin(-\phi_0)}{\sin\phi_0}\right]. \quad (3.78)$$
$$\times\int_{-\infty}^{\infty}e^{-y^2/2}dyU(-\xi)$$

Eq. (3.35), which is defined as the error function, is inserted into Eq. (3.78). When simplifying the Eq. (3.78), Eq. (3.78) can be rewritten as

$$\overrightarrow{E_{PO_2}}(P) = -\overrightarrow{e_z}\frac{\overrightarrow{E_0}}{2}\left\{\frac{n\left[\cos\left(\pi/n\right)-\sin\left\{\frac{\pi-(\beta+\phi_0)}{n}\right\}\right]}{\cos\left(\pi/n\right)-\sin\left(\pi/n\right)}\right\}e^{jk\left(x_S\cos\phi_0-R_{S_1}\right)}U(-\xi). \quad (3.79)$$

If we remember, it is clear that n is equal to 2 for a half-plane because the outer angle of a half-plane is 2π [1]. Thus, Eq. (3.79) can be rewritten as

$$\overrightarrow{E_{PO_2}}(P) = -\overrightarrow{e_z}\frac{\overrightarrow{E_0}}{2}\left\{\frac{n\left[\cos\left(\pi/n\right)-\sin\left\{\frac{\pi-(\beta+\phi_0)}{n}\right\}\right]}{\left[\cos\left(\pi/n\right)-\sin\left(\pi/n\right)\right]}\Big|_{n=2}\right\}e^{jk\left(x_s\cos\phi_0-R_{S_1}\right)}U(-\xi). \quad (3.80)$$

When Eq. (3.80) is rearranged, it is rewritten as

$$\overrightarrow{E_{PO_2}}(P) = -\overrightarrow{e_z}\overrightarrow{E_0}e^{jk\left(x_s\cos\phi_0 - R_{S_1}\right)}U(-\xi) \tag{3.81}$$

where R_{S_1} is equal to $\left[(x_s - x)\cos\phi_0 + y\sin\phi_0\right]$ according to Fig. 13.

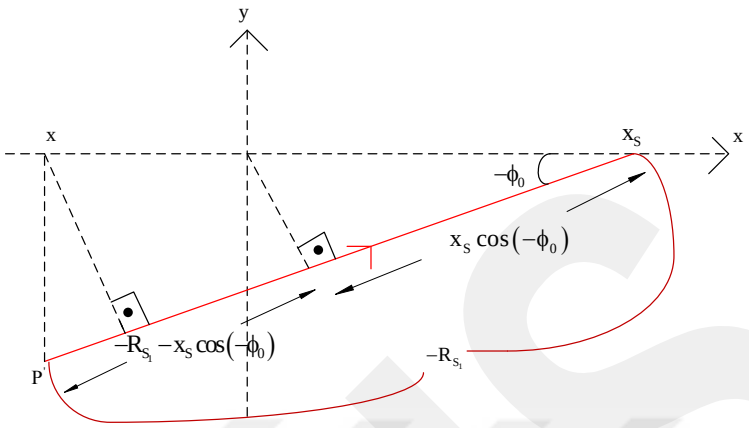

Fig. 13. The geometry of the incident part

According to Fig. 13, the equation of R_{S_1} is attached in Eq. (3.81). Hence, Eq. (3.81) can be rewritten as

$$\overrightarrow{E_{PO_2}}(P) = -\overrightarrow{e_z}\overrightarrow{E_0}e^{jk(x\cos\phi_0 + y\sin\phi_0)}U(-\xi). \tag{3.82}$$

The term of ξ can be showed in Eq. (3.68), which is the detour parameter, where $g(x_e)$ is equal to l_d, and $g(x_s)$ is equal to l_{GO} [2]. It is shown in Fig. 14.

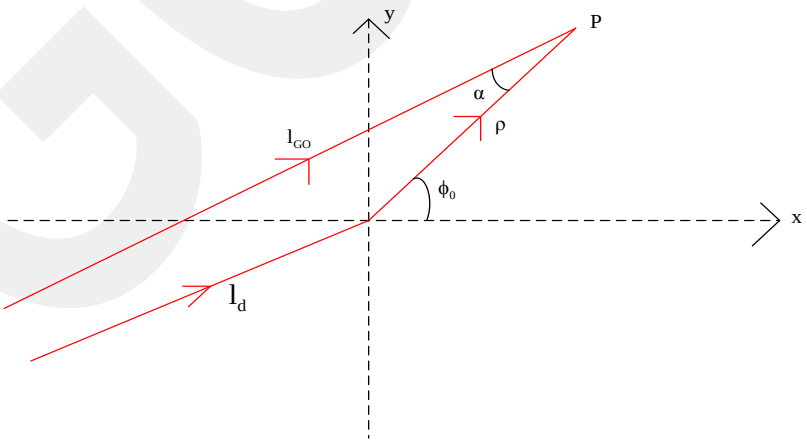

Fig. 14. The geometry of obtaining the detour parameter, ξ, for incident part

Let $g(x_e)$ is l_d, and $g(x_S)$ is l_{GO}, according to Fig. 10, l_d is equal to $(\rho + l_1)$, l_{GO} is equal to $(l_1 + x)$, and x is equal to $(\rho\cos\alpha)$, where α is equal to $\left[\pi - (\phi + \phi_0)\right]$, and $\left[l_d - l_{GO}\right]$ is equal to $\left[2\rho\cos^2\left(\frac{\phi + \phi_0}{2}\right)\right]$ according to Fig. 14. Hence, Eq. (3.70) can be rewritten as

$$\xi = -\sqrt{2\rho k}\cos\left(\frac{\phi + \phi_0}{2}\right). \tag{3.83}$$

Eq.(3.83) is inserted into Eq.(3.82). As a result, the equation of the incident part of PO equations can be obtained as

$$\overrightarrow{E_{PO_2}}(P) = -\overrightarrow{e_z}\overrightarrow{E_0}e^{jk(x\cos\phi_0 + y\sin\phi_0)}U\left(\sqrt{2\rho k}\cos\left(\frac{\phi + \phi_0}{2}\right)\right). \tag{3.84}$$

3.3. THE CONVERSION OF THE SCATTERED ELECTRIC FIELD TO GO FORM

In order to find the GO fields, the scattered electric field, which is found in Eq. (3.36), is benefited from this part. The stational phase method is applied for Eq. (3.36), where the stational phase value of R_S is defined as R_{S_1}, which is equal to $\sqrt{\left[\left(x-x_S\right)^2+y^2\right]}$.

Remind that we take into account the reflected part in order to calculate the first stational phase point, which is defined as $\alpha_{S_1}=\phi_0$. In the first stational point, x' is defined as x_s, R_S is defined as R_{S_1}, and α_s is defined as ϕ_0. Using these parameters (i.e., x_s, R_{S_1}, and ϕ_0), Eq. (3.36) can be rewritten as

$$\overrightarrow{E_{S_1}}=\overrightarrow{e_z}\frac{ke^{j\frac{\pi}{4}}\overrightarrow{E_0}}{\sqrt{2\pi}}\left\{\frac{\sin\phi_0\left(\sin\phi_0-\sin\theta\right)}{\sin\phi_0+\sin\theta}\right\}\frac{1}{\sqrt{kR_{S_1}}}e^{jk\left(x_s\cos\phi_0-R_{S_1}\right)} \times\int_{-\infty}^{\infty}e^{-jk\frac{\sin^2\phi_0}{2R_{S_1}}\left(x-x_s\right)^2}dx'U\left(-\xi\right) \quad . \quad (3.85)$$

Because y is equal to $\left(\frac{x}{\sin\phi_0}\right)$ according to Fig. 10, Eqs. (3.59), (3.60), and (3.61) are inserted into Eq. (3.85). Hence, Eq. (3.85) can be rewritten as

$$\overrightarrow{E_{S_1}}=\overrightarrow{e_z}\overrightarrow{E_0}\left[\frac{\sin\phi_0-\sin\theta}{\sin\phi_0+\sin\theta}\right]e^{jk\left(x_s\cos\phi_0-R_{S_1}\right)}U\left(\xi\right) \quad (3.86)$$

where $R_{S_1}=x_s\cos\phi_0+\rho\cos\left[\pi-\left(\phi+\phi_0\right)\right]$.

It is shown in Fig. 15.

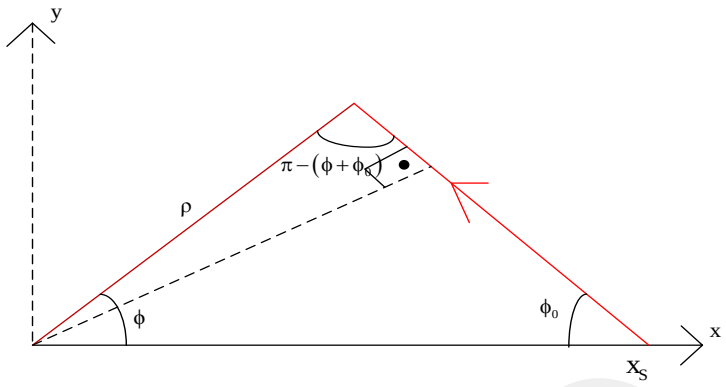

Fig.15. The geometry of R_{S_1} for reflected GO field

As a result, Eq. (3.86) can be rearranged as

$$\overrightarrow{E_{S_1}} = \overrightarrow{e_z}\overrightarrow{E_0}\left[\frac{\sin\phi_0 - \sin\theta}{\sin\phi_0 + \sin\theta}\right] e^{jk\rho\cos(\phi+\phi_0)} U(\pi - \phi_0 - \phi) \qquad (3.87)$$

for the reflected GO field.

It is clear that n, which is called as wedge angle (WA) factor, is equal to 2 for a half-plane because the outer angle of a half plane, ϕ, is equal to $2\pi = 360^\circ$ [1]. Thus, $WA = (2-n)\pi = 0$ for $n = 2$.

Using the angle values (i.e., ϕ and ϕ_0) in the graph of reflected GO field in Matlab [3], the geometry of reflected GO field is shown in Fig. 16.

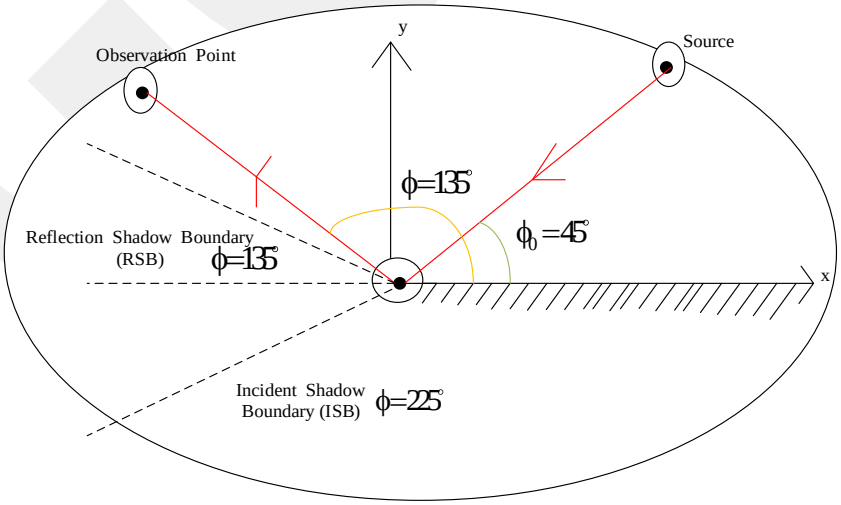

Fig.16. The geometry of the reflected GO field

Similarly, recall that we take into account the incident part in order to calculate the second stational phase point, which is defined as $\alpha_{S_2} = -\phi_0$. In the second stational point, α_s is defined as $-\phi_0$, x' is defined as x_s, and R_S is defined as R_{S_1}. Eq. (3.36) can be rewritten as

$$\overrightarrow{E_{s_2}} = \overrightarrow{e_z}\frac{ke^{j\frac{\pi}{4}}\overrightarrow{E_0}}{\sqrt{2\pi}}\int_{x'=0}^{\infty}\left[\frac{\sin^2\alpha - \sin\phi_0\sin\theta}{\sin\alpha+\sin\theta}\right]e^{jkx'\cos\phi_0}\frac{e^{-jkR_S}}{\sqrt{kR_S}}dx'. \qquad (3.88)$$

Using these parameters (i.e., x_s, R_{S_1}, and $-\phi_0$), Eq. (3.88) can be rearranged as

$$\overrightarrow{E_{s_2}} = \overrightarrow{e_z}\frac{ke^{j\frac{\pi}{4}}\overrightarrow{E_0}}{\sqrt{2\pi}}\left[\frac{\sin^2\phi_0 - \sin\phi\sin\theta}{-\sin\phi_0+\sin\theta}\right]\frac{1}{\sqrt{kR_{S_1}}}e^{jk(x_s\cos\phi_0 - R_S)} \times\int_{-\infty}^{\infty}e^{-jk\frac{\sin^2\phi_0}{2R_{S_1}}(x-x_s)^2}dx'U(\xi) \qquad (3.89)$$

Because y is equal to $\left(\frac{x}{\sin\phi_0}\right)$ according to Fig. 10, Eqs. (3.59), (3.60), and (3.61) are inserted into Eq. (3.89). Hence, Eq. (3.89) can be rewritten as

$$\overrightarrow{E_{s_2}} = -\overrightarrow{e_z}\overrightarrow{E_0}e^{jk\left(x_s\cos\phi_0 - R_{S_1}\right)}U(\xi) \qquad (3.90)$$

where $R_{S_1} = x_s\cos\phi_0 + \rho\cos\left[\pi - (\phi - \phi_0)\right]$.

It is shown in Fig. 17.

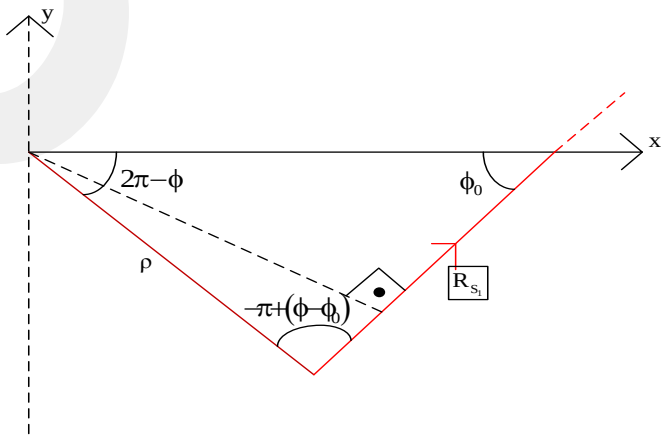

Fig.17. The geometry Of R_{S_1} for incident GO field

As a result, Eq. (3.90) can be rearranged as

$$\overrightarrow{E_{S_2}} = -\overrightarrow{e_z}\overrightarrow{E_0}e^{jk\rho\cos(\phi-\phi_0)}U(\phi-\pi-\phi_0) \tag{3.91}$$

for the incident GO field.

Using the angle values (i.e., ϕ and ϕ_0) in the graph of incident GO field in Matlab [3], the geometry of incident GO field is shown in Fig. 18.

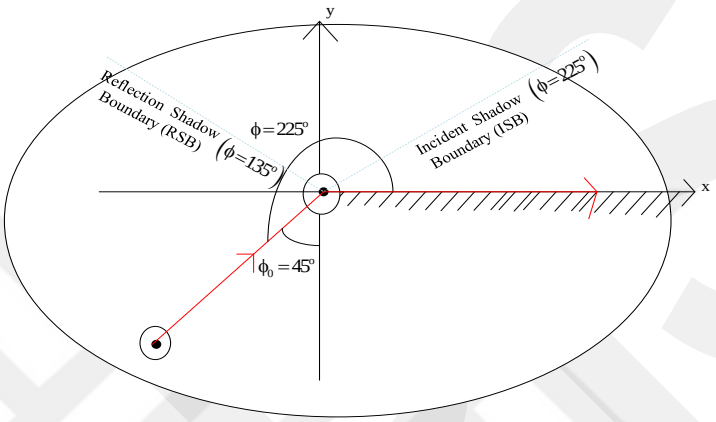

Fig.18. The Geometry Of The Incident GO Field

In conclusion, the total GO field can be obtained as

$$\overrightarrow{E_{TGO}} = \overrightarrow{e_z}\overrightarrow{E_0}\left[e^{jk\rho\cos(\phi-\phi_0)}U(\pi+\phi_0-\phi)+\left(\frac{\sin\phi_0-\sin\theta}{\sin\phi_0+\sin\theta}\right)e^{jk\rho\cos(\phi+\phi_0)}U(\pi-\phi_0-\phi)\right] \tag{3.92}$$

where $\left\{\overrightarrow{e_z}\overrightarrow{E_0}e^{jk\rho\cos(\phi-\phi_0)}U(\pi+\phi_0-\phi)\right\}$ is defined as the incident GO field, and $\left\{\overrightarrow{e_z}\overrightarrow{E_0}\left(\frac{\sin\phi_0-\sin\theta}{\sin\phi_0+\sin\theta}\right)e^{jk\rho\cos(\phi+\phi_0)}U(\pi-\phi_0-\phi)\right\}$ is defined as the reflected GO field. In addition, using the graph of total GO field in Matlab [2,3], the geometry of the total GO field is shown in Fig. 19.

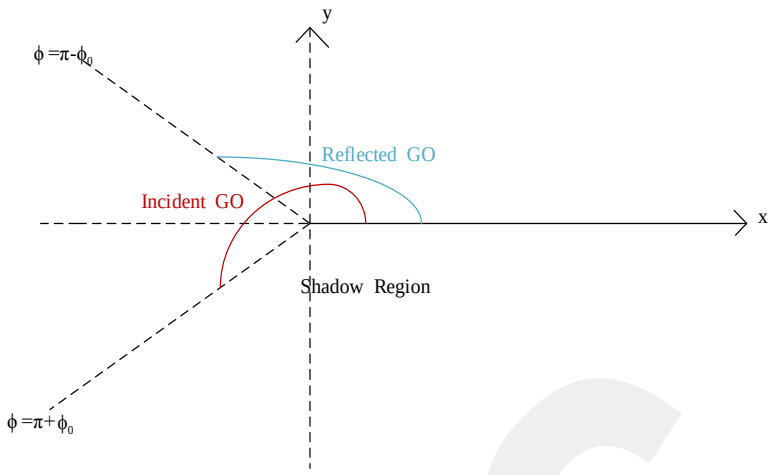

Fig. 19. The Geometry Of The Total GO Field

3.4. THE APPLICATION OF THE EDGE POINT METHOD TO THE SCATTERED FIELD EQUATION AND OBTAINING THE EQUATIONS OF THE DIFFRACTED FIELD AND THE TOTAL FIELD

In this section, we will apply the edge point method to the expression of the scattered electric field which is obtained after applying the stationary phase method. Since the integral spacing of this expression consists of discontinuous points, the edge point method is applied to the expression of scattered electric field. In the edge point method, calculation is made at the edge point of the integral. Using the edge point method, the edge diffracted field, $\overrightarrow{E_d}$, can be calculated by using the formula

$$\int_0^{\infty} f(x) e^{jk\gamma(x)} dx \approx \mp \overrightarrow{e_z} \frac{1}{jk} \frac{f(0)}{\gamma'(0)} e^{jk\gamma(0)} \tag{3.93}$$

where $f(0)$ and $\gamma(0)$ denote the values of the amplitude and the phase functions of Eq. (3.88) at the edge point, respectively, and $g'(0)$ is the value of the first derivative of the phase function at the edge point [7]. When the edge point is the upper value of the integral, the minus sign in Eq. (3.93) is used but the plus sign is used for the lower limit [7]. Since the upper value of the integral in Eq. (3.36), the minus sign in Eq. (3.93) should be used.

When the minus sign of Eq. (3.93) is inserted into Eq. (3.88), the equation can be obtained as

$$\overrightarrow{E_d} = \frac{-1}{jk} \frac{k e^{j\frac{\pi}{4}} \overrightarrow{E_0}}{\sqrt{2\pi}} \left(\frac{\sin^2\phi - \sin\phi_0 \sin\theta}{\sin\phi + \sin\theta} \right) \frac{1}{\sqrt{kR_e}} \left(\frac{1}{\cos\phi + \cos\phi_0} \right) e^{-jkR_e} \tag{3.94}$$

where R_e is equal to ρ, α is equal to $(\pi - \phi)$, and $\left(g'(x') = \cos\phi - \cos\alpha\right)$ at the edge point according to Fig. 20 [2].

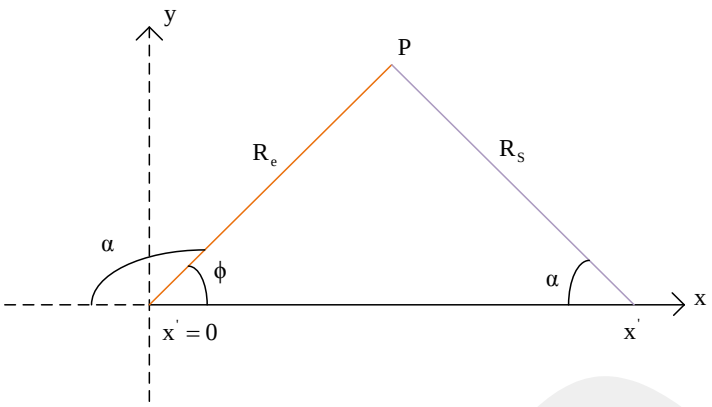

Fig. 20. The Geometry Of The EP Method

Eq. (3.94) can be rewritten as

$$\overrightarrow{E_d} = -\frac{e^{j\frac{\pi}{4}}}{\sqrt{2\pi}}\overrightarrow{E_0}\left(\frac{\sin^2\phi - \sin\phi_0 \sin\theta}{\sin\phi + \sin\theta}\right)\left(\frac{1}{\cos\phi + \cos\phi_0}\right)\frac{e^{-jk\rho}}{\sqrt{k\rho}}. \qquad (3.95)$$

In order to make Uniform in Eq. (3.95), the equation of $\overrightarrow{E_d}$ is both multiplied and divided by $\left(2\sin\frac{\phi}{2}\sin\frac{\phi_0}{2}\right)$. Hence, Eq. (3.95) can be rewritten as

$$\overrightarrow{E_d} = -\frac{e^{-j\frac{\pi}{4}}}{\sqrt{2\pi}}\overrightarrow{E_0}\left(\frac{\sin^2\phi - \sin\phi_0 \sin\theta}{\sin\phi + \sin\theta}\right)\left(\frac{1}{\cos\phi + \cos\phi_0}\right)\frac{e^{-jk\rho}}{\sqrt{k\rho}}\left(\frac{2\sin\frac{\phi}{2}\sin\frac{\phi_0}{2}}{2\sin\frac{\phi}{2}\sin\frac{\phi_0}{2}}\right). \qquad (3.96)$$

Eq. (3.96) can be rearranged as

$$\overrightarrow{E_d} = \overrightarrow{E_0}\left(\frac{\sin^2\phi - \sin\phi_0 \sin\theta}{\sin\phi + \sin\theta}\right)\left(\frac{1}{2\sin\frac{\phi}{2}\sin\frac{\phi_0}{2}}\right)\left[\frac{e^{-j\frac{\pi}{4}}}{\sqrt{2\pi}}\left(\frac{2\sin\frac{\phi}{2}\sin\frac{\phi_0}{2}}{\cos\phi + \cos\phi_0}\right)\frac{e^{-jk\rho}}{\sqrt{k\rho}}\right]. \qquad (3.97)$$

The trigonometric relations of

$$\left[\frac{2\sin\frac{\phi}{2}\sin\frac{\phi_0}{2}}{\cos\phi + \cos\phi_0}\right] = \left[\frac{\cos\left(\frac{\phi - \phi_0}{2}\right) - \cos\left(\frac{\phi + \phi_0}{2}\right)}{2\cos\left(\frac{\phi - \phi_0}{2}\right)\cos\left(\frac{\phi + \phi_0}{2}\right)}\right] \qquad (3.98)$$

is used for Eq. (3.97) [2]. Eq. (3.98) is inserted into Eq. (3.97). Therefore, Eq. (3.97) can be rewritten as

$$\overrightarrow{E_d}=\overrightarrow{E_0}\left\{\frac{\sin^2\phi-\sin\phi_0\sin\theta}{\sin\phi+\sin\theta}\right\}\left(\frac{1}{2\sin\frac{\phi}{2}\sin\frac{\phi_0}{2}}\right)\left[\frac{e^{-j\frac{\pi}{4}}}{2\sqrt{2\pi}}\left(\frac{-1}{\cos\left(\frac{\phi+\phi_0}{2}\right)}-\frac{1}{\cos\left(\frac{\phi-\phi_0}{2}\right)}\right)\frac{e^{-jk\rho}}{\sqrt{k\rho}}\right]. \quad (3.99)$$

In addition, the formula of detour parameter is benefited in order to uniform in Eq. (3.99). Eq. (3.70) and Eq. (3.83) are inserted into Eq. (3.99), respectively. Thus, Eq. (3.99) can be rearranged as

$$\overrightarrow{E_d}=\overrightarrow{E_0}\left\{\frac{\sin^2\phi-\sin\phi_0\sin\theta}{\sin\phi+\sin\theta}\right\}\left(\frac{1}{2\sin\frac{\phi}{2}\sin\frac{\phi_0}{2}}\right)\left[\frac{e^{-j\frac{\pi}{4}}}{2\sqrt{\pi}}\frac{1}{\left(-\sqrt{2k\rho}\cos\left(\frac{\phi-\phi_0}{2}\right)\right)}e^{-j\left[\xi_-^2+kl\right]}\right. \quad .(3.100)$$

$$\left.-\frac{e^{-j\frac{\pi}{4}}}{2\sqrt{\pi}}\frac{1}{\left(-\sqrt{2k\rho}\cos\left(\frac{\phi+\phi_0}{2}\right)\right)}e^{-j\left[\xi_+^2+kl\right]}\right]$$

Using the equation of

$$\text{sign}\alpha(x)F\left[|x|\right]\sim\frac{e^{-j\frac{\pi}{4}}}{2\sqrt{\pi}}\frac{e^{-jx^2}}{x} \quad (3.101)$$

is used for Eq.(3.100) [2]. Therefore, Eq. (3.100) can be rewritten as

$$\overrightarrow{E_d}=-\overrightarrow{E_0}\left(\frac{\sin^2\phi-\sin\phi_0\sin\theta}{\sin\phi_0+\sin\theta}\right)\left(\frac{1}{2\sin\frac{\phi}{2}\sin\frac{\phi_0}{2}}\right)\left[e^{jk\rho\cos(\phi-\phi_0)}\,\text{sign}(\xi_-)F\left[|\xi_-|\right]\right. . \quad (3.102)$$

$$\left.-e^{jk\rho\cos(\phi+\phi_0)}\text{sign}(\xi_+)F\left[|\xi_+|\right]\right]$$

In this manner, by obtaining Eq. (3.102), the equation of diffracted field is found. After obtaining the equation of the diffracted field, since we know the equation of the total GO field, the equation of the total field can be written. As a result, using Eq. (3.92) and Eq. (3.102), the equation of the total field can be written as

$$\overrightarrow{E_T}=\overrightarrow{E_{TGO}}+\overrightarrow{E_d}. \quad (3.103)$$

3.5. THE CONVERSION OF THE SCATTERED FIELD EQUATION IN THE HALF- PLANE TO THE WEDGE

As mentioned before, the equation of the scattered field in half-plane is obtained in Eq. (3.36). It is possible to convert into the wedge form. In this part, since we deal with the soft surface in this thesis, the expression of Eq. (3.42) in half-plane will be converted to the wedge form. At the present time, a wedge is taken into account in Fig. 7 and Fig. 21 [1,11].

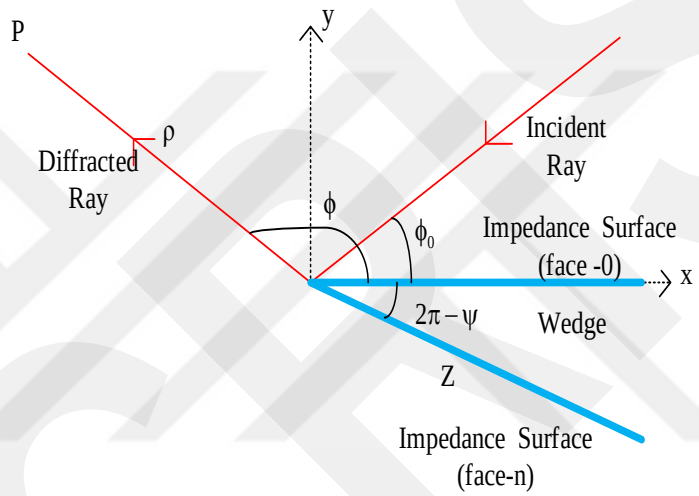

Fig. 21. The Geometry Of The Wedge Diffraction With Two Impedance Faces

According to Fig. 21, a wedge has two same boundary conditions, which are defined as impedance surfaces. The cylindrical coordinates are given by (ρ,ϕ,z). According to Fig. 21, ϕ_0 is the angle of incidence, Z is the surface impedance, P is the observation point, and ψ is the outer angle of wedge. The parameter of n is defined as $\left(\frac{\psi}{\pi}\right)$. As mentioned before, since the outer angle of a half-plane, ψ, 2π, n is equal to 2 for a half-plane [1]. The PO integrals is used to solve the wedge diffraction problem. With this information in mind, the cotangent function in Eq. (3.45) for the wedge diffraction [1]. As mentioned before, because the soft surface is emphasized on this thesis, the

cotangent function in the integrand of Eq. (3.45), which is equal to $\left\{\cot g\frac{\beta-\phi_0}{2}=\sin\left(\pi/n\right)\frac{\cos\left(\pi/n\right)-\sin\left\{\frac{\pi-(\beta-\phi_0)}{n}\right\}}{\cos\left(\pi/n\right)-\cos\left\{\frac{\pi-(\beta-\phi_0)}{n}\right\}}\Big|_{n=2}\right\}$, will be used.

As a result, the PO integrals can be rewritten as

$$\overrightarrow{E_{PO_1}}=\vec{e}_z\frac{ke^{j\frac{\pi}{4}}\overrightarrow{E_0}}{2\sqrt{2\pi}}\int_{x'=0}^{\infty}\left[\frac{y}{R_S}\frac{\sin\alpha-\sin\phi_0\sin\theta}{\sin\alpha+\sin\theta}\right]\left[\sin\left(\pi/n\right)\frac{\cos\left(\pi/n\right)-\sin\left\{\frac{\pi-(\beta-\phi_0)}{n}\right\}}{\cos\left(\pi/n\right)-\cos\left\{\frac{\pi-(\beta-\phi_0)}{n}\right\}}\Big|_{n=2}\right] \tag{3.104}$$
$$\times\left(\frac{\cos\phi_0-\cos\beta}{\sin\phi_0}\right)e^{jkx'\cos\phi_0}\frac{e^{-jkR_S}}{\sqrt{kR_S}}dx'$$

and

$$\overrightarrow{E_{PO_2}}=-\vec{e}_z\frac{ke^{j\frac{\pi}{4}}\overrightarrow{E_0}}{2\sqrt{2\pi}}\int_{x'=0}^{\infty}\left[\frac{y}{R_S}\frac{\sin\alpha-\sin\phi_0\sin\theta}{\sin\alpha+\sin\theta}\right]\left[\sin\left(\pi/n\right)\frac{\cos\left(\pi/n\right)-\sin\left\{\frac{\pi-(\beta+\phi_0)}{n}\right\}}{\cos\left(\pi/n\right)-\cos\left\{\frac{\pi-(\beta+\phi_0)}{n}\right\}}\Big|_{n=2}\right] \tag{3.105}$$
$$\times\left(\frac{\cos\phi_0-\cos\beta}{\sin\phi_0}\right)e^{jkx'\cos\phi_0}\frac{e^{-jkR_S}}{\sqrt{kR_S}}dx'$$

for the parts of reflected and incident, respectively. Again, the coefficient of $\left[\sin\left(\pi/n\right)\frac{\cos\left(\pi/n\right)-\sin\left\{\frac{\pi-(\beta\mp\phi_0)}{n}\right\}}{\cos\left(\pi/n\right)-\cos\left\{\frac{\pi-(\beta\mp\phi_0)}{n}\right\}}\Big|_{n=2}\right]$ in the parts of reflected and incident PO integral will be multiplied by the expression of $\left(\frac{\mp1}{\cos\left(\pi/n\right)-\sin\left(\pi/n\right)}\right)$.

The aim is to eliminate this above coefficient because the coefficient needs the value of 1 in the stational phase method. In this manner, the parts of reflected and incident PO integral in half-plane are converted to the form of wedge. Eqs. (104) and (105) can be rewritten as

$$\overrightarrow{U_{PO_1}}(P)=\overrightarrow{e_z}\frac{ke^{j\frac{\pi}{4}}\overrightarrow{E_0}}{2\sqrt{2\pi}}\int_{x'=0}^{\infty}\left[\frac{\frac{y}{R_S}\sin\alpha-\sin\phi_0\sin\theta}{\sin\alpha+\sin\theta}\right](f_-)\times\left(\frac{\cos\phi_0-\cos\beta}{\sin\phi_0}\right)e^{jkx'\cos\phi_0}\frac{e^{-jkR_S}}{\sqrt{kR_S}}dx' \quad (3.106)$$

and

$$\overrightarrow{U_{PO_2}}=-\overrightarrow{e_z}\frac{ke^{j\frac{\pi}{4}}\overrightarrow{E_0}}{2\sqrt{2\pi}}\int_{x'=0}^{\infty}\left[\frac{\frac{y}{R_S}\sin\alpha-\sin\phi_0\sin\theta}{\sin\alpha+\sin\theta}\right](f_+)\left(\frac{\cos\phi_0-\cos\beta}{\sin\phi_0}\right)\times e^{jkx'\cos\phi_0}\frac{e^{-jkR_S}}{\sqrt{kR_S}}dx' \quad (3.107)$$

for the parts of reflected and incident PO integral, respectively. According to Eq.(3.106), (f_-) is equal to $\left[\sin\left(\frac{\pi}{n}\right)\frac{\cos\left(\frac{\pi}{n}\right)-\sin\left\{\frac{\pi-(\beta\mp\phi_0)}{n}\right\}}{\cos\left(\frac{\pi}{n}\right)-\cos\left\{\frac{\pi-(\beta\mp\phi_0)}{n}\right\}}\Big|_{n=2}\right]$ multiplied by $\left(\frac{-1}{\cos\left(\frac{\pi}{n}\right)-\sin\left(\frac{\pi}{n}\right)}\right)$, and (f_+) is equal to $\left[\sin\left(\frac{\pi}{n}\right)\frac{\cos\left(\frac{\pi}{n}\right)-\sin\left\{\frac{\pi-(\beta\mp\phi_0)}{n}\right\}}{\cos\left(\frac{\pi}{n}\right)-\cos\left\{\frac{\pi-(\beta\mp\phi_0)}{n}\right\}}\Big|_{n=2}\right]$ multiplied by $\left(\frac{+1}{\cos\left(\frac{\pi}{n}\right)-\sin\left(\frac{\pi}{n}\right)}\right)$.

Note that Eq. (3.45) directly reduces to Eq. (3.44) for n=2 [1].

In conclusion, the PO integrals in the wedge form can be obtained as

$$\overrightarrow{U_{PO_{(1,2)}}}(P)=\overrightarrow{e_z}\frac{ke^{j\frac{\pi}{4}}\overrightarrow{E_0}}{2\sqrt{2\pi}}\left[\begin{array}{l}\int_{x'=0}^{\infty}\left[\frac{\frac{y}{R_S}\sin\alpha-\sin\phi_0\sin\theta}{\sin\alpha+\sin\theta}\right](f_-)\left(\frac{\cos\phi_0-\cos\beta}{\sin\phi_0}\right)\\ \times e^{jkx'\cos\phi_0}\frac{e^{-jkR_S}}{\sqrt{kR_S}}dx'+\int_{x'=0}^{\infty}\left[\frac{\frac{y}{R_S}\sin\alpha-\sin\phi_0\sin\theta}{\sin\alpha+\sin\theta}\right](f_+)\left(\frac{\cos\phi_0-\cos\beta}{\sin\phi_0}\right)e^{jkx'\cos\phi_0}\frac{e^{-jkR_S}}{\sqrt{kR_S}}dx'\end{array}\right]. \quad (3.108)$$

Eq. (3.108) makes possible one to evaluate the wedge diffracted waves with the PO integral.

3.6. ASYMPTOTIC EVALUATION OF PO INTEGRAL

In this section, the wedge diffracted fields of PO will be obtained by the uniform asymptotic evaluation of Eq. (3.108) [1]. At the edge point, β and R are equal to $(\pi-\phi)$ and ρ with respect to Fig. 7, and Fig. 21, respectively. In Ref [1], The uniform wedge waves of PO can be written as

$$U_{PO}=(h_{-})\,\mathrm{sign}(\xi_{-})\,F[|\xi_{-}|]-(h_{+})\,\mathrm{sign}(\xi_{+})\,F[|\xi_{+}|] \tag{3.109}$$

where $h_{\mp}$ can be explained as

$$h_{\mp}=\frac{\overrightarrow{u_0}\,2\sin(\pi/n)}{n}e^{jk\rho\cos(\phi\mp\phi_0)}\cos\left(\frac{\phi+\phi_0}{2}\right)\left(\frac{\mp1}{\cos(\pi/n)-\sin(\pi/n)}\right)\left[\frac{\cos(\pi/n)-\sin\left\{\frac{(\phi\mp\phi_0)}{n}\right\}}{\cos(\pi/n)-\cos\left\{\frac{(\phi+\phi_0)}{n}\right\}}\right] \tag{3.110}$$

according to Eq. (108). $\mathrm{sign}(x)$, which is called as the signum function, is equal to one for $x>0$ and -1 otherwise. The formula of $F[x]$, which is called as the Fresnel function, can be written as

$$F[x]=\frac{e^{j\frac{\pi}{4}}}{\sqrt{\pi}}\int_{x}^{\infty}e^{(-jt^2)}dt\,. \tag{3.111}$$

The parameter of $\xi_{\pm}$, which is called the detour parameter, can be obtained in Eq. (3.70), and Eq. (3.83).

According to the method of PO, the surface current is equal to zero at $\phi=\psi$ because the upper face of the wedge is enlightened. Hence, the scattered fields of PO by the wedge can be acquired for $n=2$. According to the specific case of Eq. (3.109) for $n=2$, the uniform scattered fields can be directly written as

$$U_{PO_c}=h_{-}|_{n=2}\,\mathrm{sign}(\xi_{-})\,F[|\xi_{-}|]-h_{+}|_{n=2}\,\mathrm{sign}(\xi_{+})\,F[|\xi_{+}|] \tag{3.112}$$

for the classical PO. By applying the stationary phase method to the incident and reflected GO fields in chapter 3.3, the total GO field was obtained.

As a result, the GO fields can be rewritten as

$$U_{GO} = u_0 \left[e^{jk\rho\cos(\phi-\phi_0)} U(-\xi_-) - \left(\frac{\sin\phi_0 - \sin\theta}{\sin\phi_0 + \sin\theta} \right) e^{jk\rho\cos(\phi+\phi_0)} U(-\xi_+) \right] \qquad (3.113)$$

where the coefficient of $\left(\frac{\sin\phi_0 - \sin\theta}{\sin\phi_0 + \sin\theta} \right)$ is the reflection coefficient (R) in impedance surface, and $U(x)$, which is called as the unit step function, is equal to one for $x > 0$ and zero otherwise.

CHAPTER 4

NUMERICAL RESULTS

In this section, the numerical analysis of the field expressions, which is involved in $\overrightarrow{E_S}$, $\overrightarrow{E_{PO_1}}$ and $\overrightarrow{E_{PO_2}}$, $\overrightarrow{E_{TGO}}$, $\overrightarrow{E_d}$, $\overrightarrow{E_T}$, and $\overrightarrow{U_{PO_{(1,2)}}(P)}$ on the half-plane and the wedge, will be examined. In order to investigate the PO method to impedance wedge diffraction, because of PO, the values of (x'), R, and β are defined as $(a\sin ir + (i.*delta))$, $(sqrt((rho.\hat{}2)+(t.\hat{}2)-(2.*rho.*t.*cos(fi))))$, and $(a\sin(rho.*\sin(fi)./R))$ in Matlab code, respectively. R is the distance between the source point to the observation point. β is the angle between the reflected ray and impedance half-plane. The value of the scatterer's size should be larger than the value of the wavelength of incident wave because of the high frequency asymptotic techniques. Hence, ρ will be taken 6λ for the situation of the high frequency techniques. The value of the angle of reflected field, which is θ, will be changed.

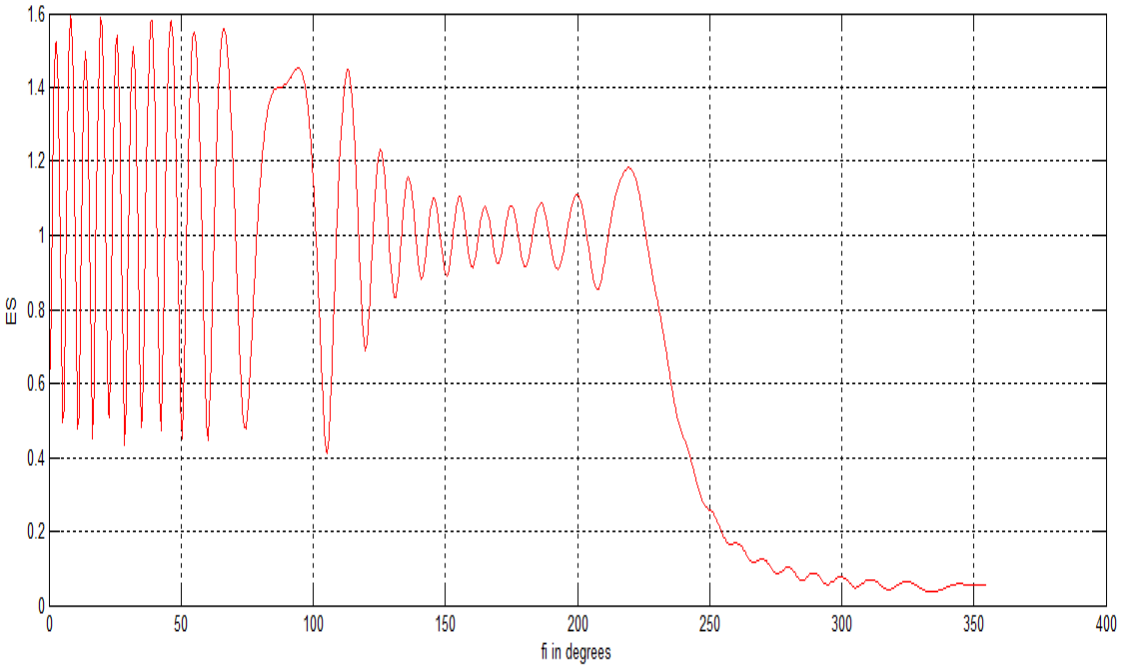

Fig.22. The Scattered Electric Fields from impedance half-plane.

Figure 22 shows the scattered field $\overrightarrow{E_S}$, which is expressed in Eq. (3.36), from impedance half-plane, and the variation of Eq. (3.36) versus the observation angle, ϕ. The scattered field integral does not deviate after $(\phi = \pi + \phi_0)$ because the scattered electric field progresses as the reflected field, perpendicularly. The diffracted fields and the reflected fields are involved in the PO scattered field. Because the impedance half-plane is examined, the value of ϕ is between 0° and 360°. However, since a deviation of 360° is observed, the deviation is eliminated by ending the angle ϕ at the value of $\left(355 \times \pi/180\right)$ in the Matlab. ϕ_0 is the angle of incidence. The amplitude value of θ is equal to between 1.4 and 1.6 in reflected field, the angle range of oscillating waves advance increasing and decreasing between 0° and 220°. After 220° in Fig. 22, the wave decreases suddenly. From 250° to 355°, the wave progresses by oscillating, and it is damped at 355° because of the deviation.

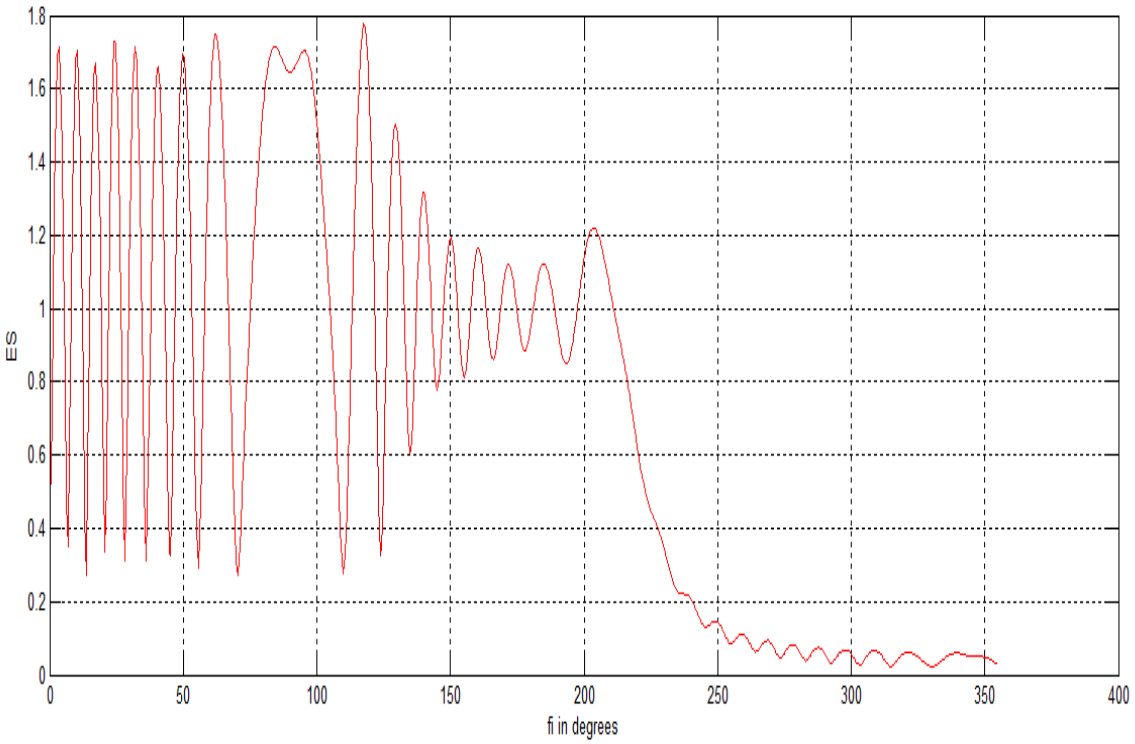

Fig. 23. The Scattered Electric Field on impedance half-plane according to the variations of the incident and reflected angle values.

Figure 23 indicates that as the angles of the incidence and reflected are reduced (i.e., the reflected angle is asin(4) instead of asin(3), and the angle of incidence is $\left(45^{\circ}\right)$ instead of $\left(60^{\circ}\right)$ in Matlab), the amplitude range value of the reflected field increases from 1.6 to between about 1.6 and 1.8. Like Fig. 22, since a deviation of 360° is observed, the deviation is eliminated by ending the angle ϕ at the value of $\left(355\times\pi/180\right)$ in the Matlab for obtaining Fig. 23. Unlike Fig. 22, the angle range of oscillating waves advance increasing and decreasing between 0° and 204°, and after 204°, the wave decreases suddenly. From 240° to 355°, the wave progresses by oscillating, and it is damped at 355° because of the deviation.

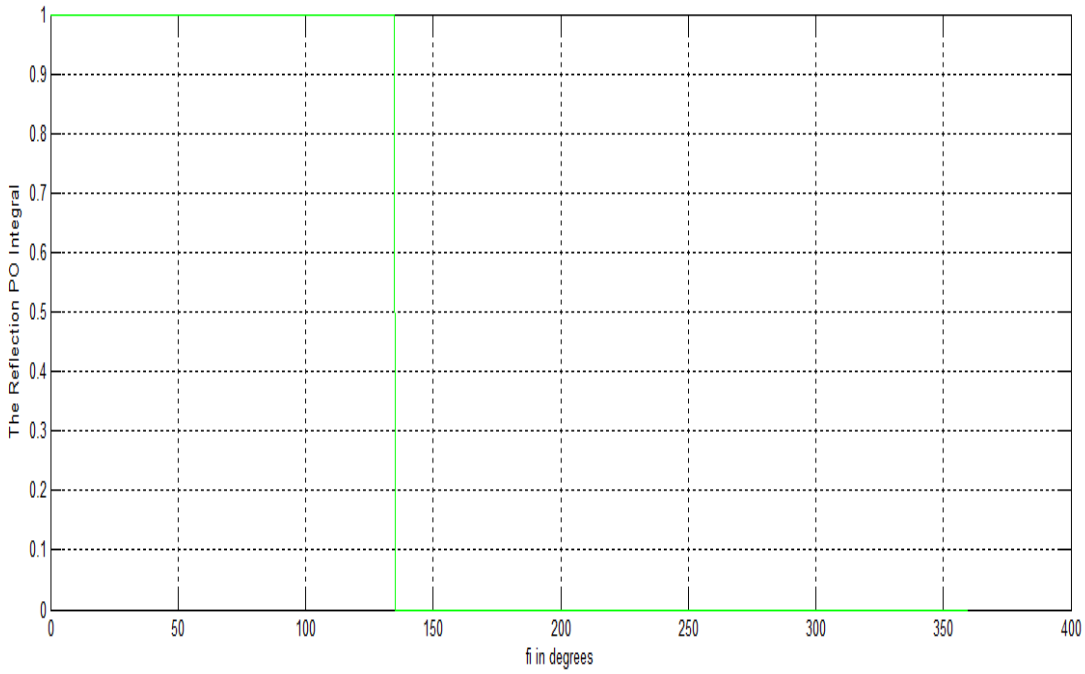

Fig. 24. The reflected part of the PO equation.

Figure 24 shows the reflected part of the PO equation, which is expressed in Eq. (3.71), from impedance half-plane. As can be seen in Fig. 24, when the part of PO, which is reflected on the impedance half-plane, reaches 135° (i.e., $(\pi-\phi_0)$, it becomes discontinuous here. From this point of view, 135° is expressed as the reflection boundary and the angle of incidence ϕ_0, is 45°.

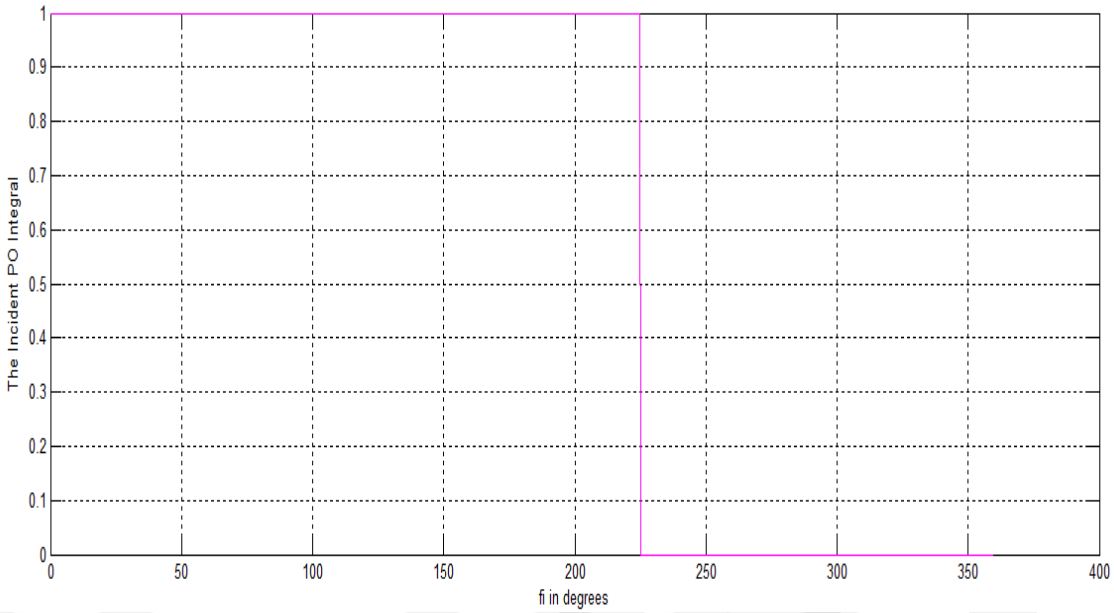

Fig. 25. The incident part of the PO equation.

Figure 25 shows the incident part of the PO equation, which is expressed in Eq. (3.84), from impedance half-plane. As can be seen in Fig. 25, when the incident part of PO on the impedance half-plane, reaches 225° (i.e., $(\pi+\phi_0)$), is expressed as the shadow boundary. From this point of view, the deviation angle, ϕ_0, is 45°.

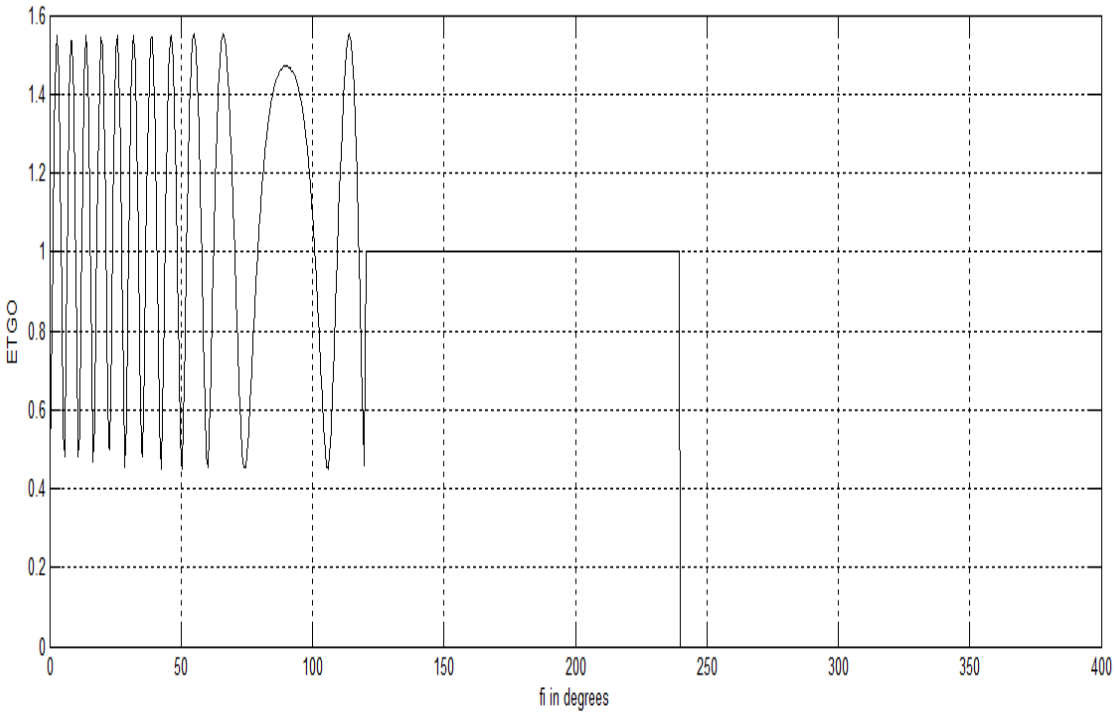

Fig. 26. The total GO field on impedance half-plane.

Figure 26 shows the total GO electric field, which consists of the incident GO and the reflected GO, on the impedance half-plane. The total GO electric field is expressed in Eq. (3.92). In Fig. 26, the angle between about 0° and 240° gives the total of incident GO and reflected GO, and the angle between about 240° and 360° gives the shadow region.

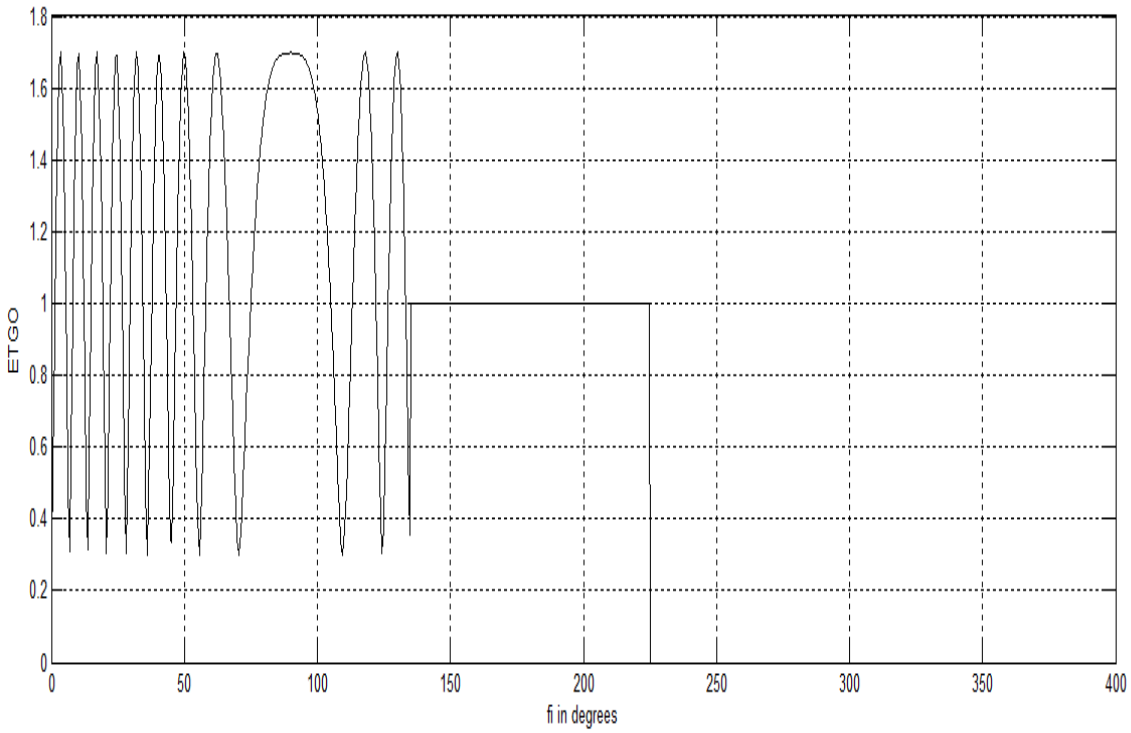

Fig. 27. The total GO fields on impedance half-plane according to the variations of the incident and reflected angle values.

Figure 27 indicates that as the angles of the incident and reflected are decreased (i.e., the reflected angle is asin(4) instead of asin(3), and the angle of incidence is $\left(45^{\circ}\right)$ instead of $\left(60^{\circ}\right)$ in Matlab), the amplitude of the reflected field increases from between 1.4 and 1.6 to between about 1.6 and 1.8, the total of incident GO and reflected GO are reduced the range values between 0° to 225°, and the range angle of the shadow region is rised between 225° and 360°.

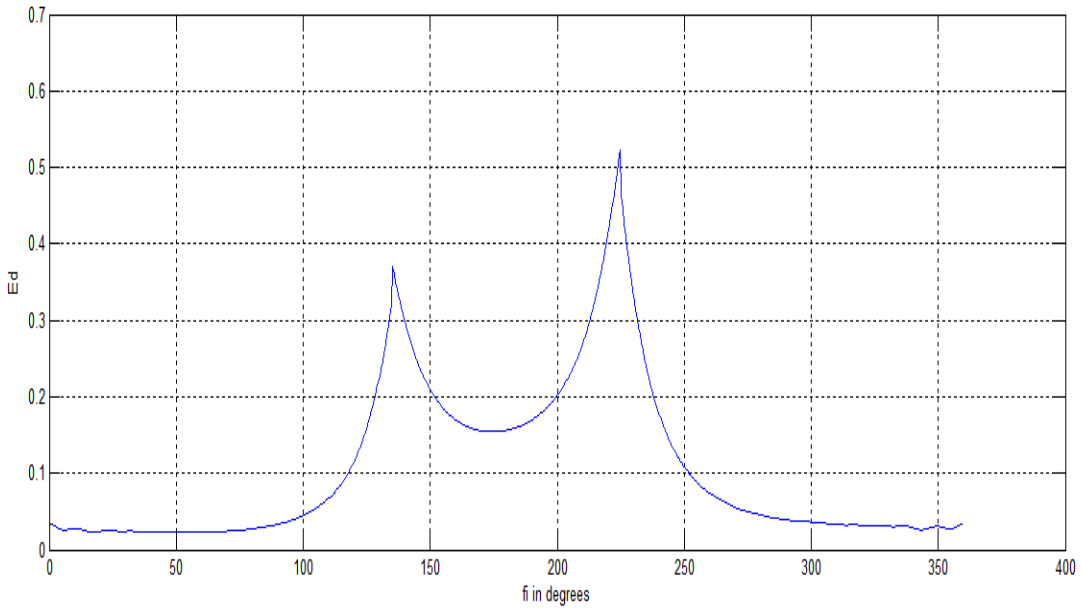

Fig. 28. The diffracted field from impedance half-plane

Figure 28 shows the diffracted field with respect to the observation angle, ϕ. The diffracted field is expressed in Eq. (3.102). As in the other obtained graphs in Matlab, in Fig. 28, the distance of observation (ρ) is defined as 6λ where λ is the wavelength. While the outer angle of the wedge (ψ) is equal to 330°, the angle of incidence (ϕ_0) is equal to 60°. The extended PO approaches to the exact solution between the angles of 135° and 225° when the angle of incidence, ϕ_0, is taken as 45° and the reflected angle, θ, is taken as asin(4) in Matlab.

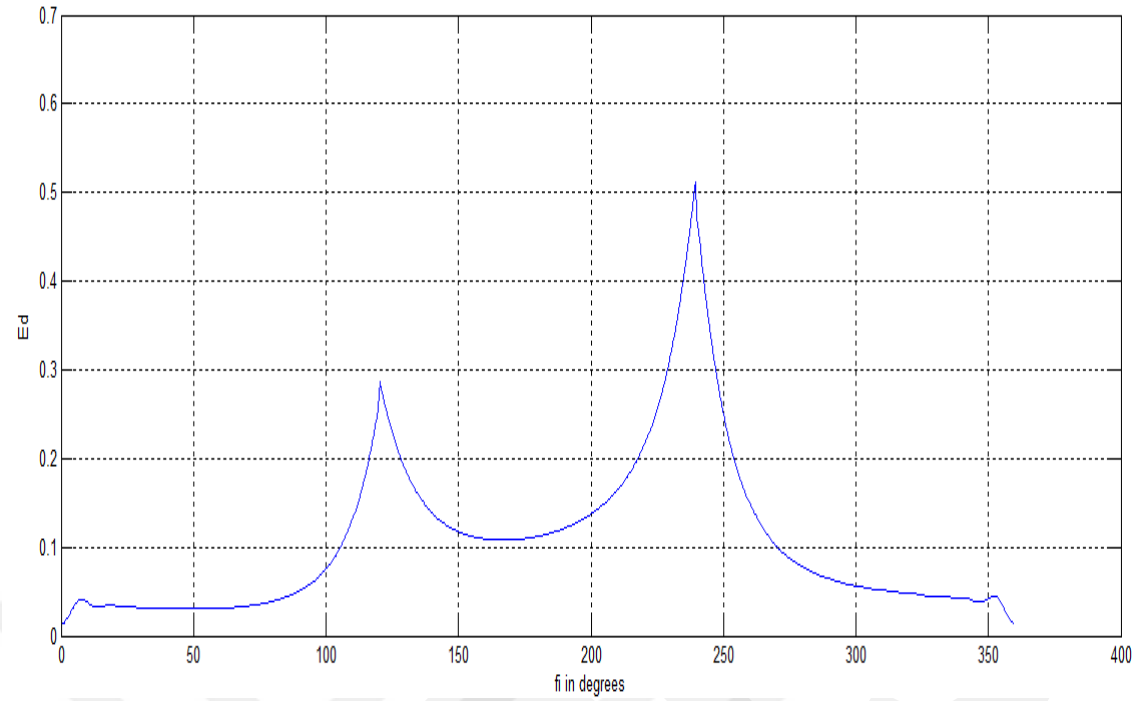

Fig. 29. The diffracted field from impedance half-plane according to the variations of the incident and reflected angle values.

Figure 29 depicts the diffracted field with respect to the observation angle, ϕ, with respect to the variations of the incident and reflected angle values. Unlike Fig. 28, according to the observation angle, as the value of incident angle decreases, the value of reflected angle increases. The extended PO approaches to the exact solution between the angles of 120° and 239° when the angle of incidence, ϕ_0, is taken as 60° and the reflected angle, θ, is taken as asin(3) in Matlab. In this manner, the range value of the extended PO is grown further.

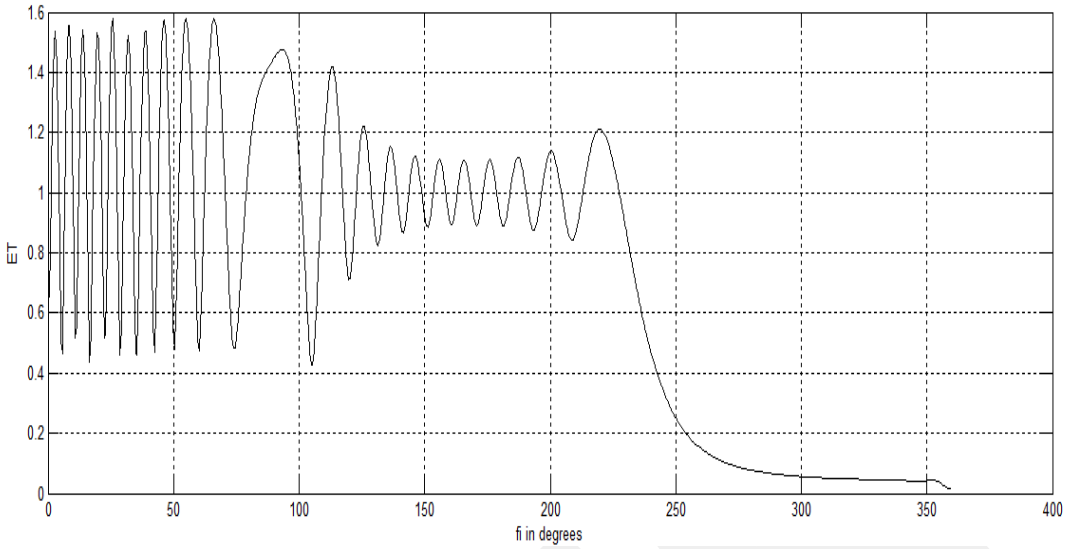

Fig. 30. The total of the reflected and diffracted fields from impedance half-plane.

Figure 30 depicts the variations of the total of the reflected and diffracted fields $(\beta = \phi_0)$ versus the observation angle, ϕ. The total of the reflected and diffracted fields is expressed in Eq. (3.103). Unlike the graph of the scattered electric field, $\overrightarrow{E_S}$, the PO integral deviates from the exact asymptotic solution after $(\phi = \pi + \phi_0)$ because the edge diffraction field is not the exact field. The amplitude value of θ is equal to between 1.4 and 1.6 in reflected field, the angle range of oscillating waves advance increasing and decreasing between 0° and 205° when the angle of incidence, (ϕ_0), is defined as 60°, and the reflected angle, θ, is defined as asin(3) in Matlab. After 220° in Fig. 30, the wave decreases suddenly, approaches zero and moves steadily down to 360°.

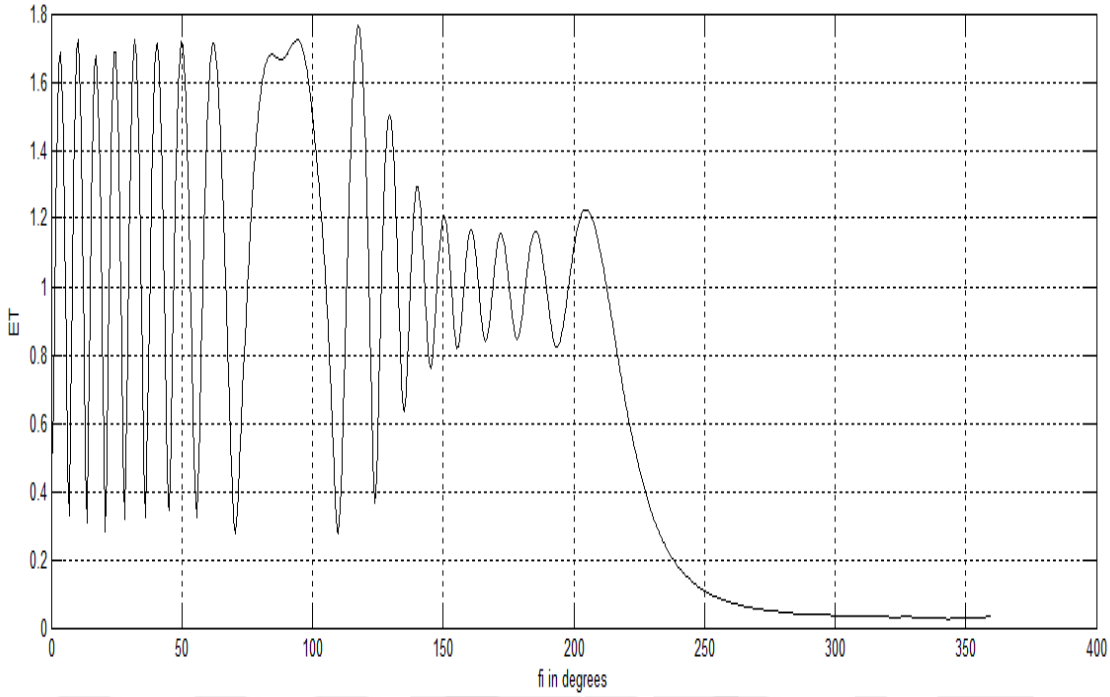

Fig. 31. The total of the reflected and diffracted fields from impedance half-plane according to the variations of the incident and reflected angle values.

Figure 31 shows the total of the reflected and diffracted fields from impedance half-plane according to the variations of the incident and reflected angle values. The amplitude value of θ, which is equal to between about 1.6 and 1.8, changes in the reflected field , the angle range of oscillating waves advance increasing and decreasing between 0° and 205° unlike Fig. 30 when the values of θ and ϕ_0, which is equal to asin(4) and 45°, respectively, is changed in Matlab. After 205° in Fig. 31, the wave decreases suddenly, approaches zero and moves steadily up to 360° unlike Fig. 30.

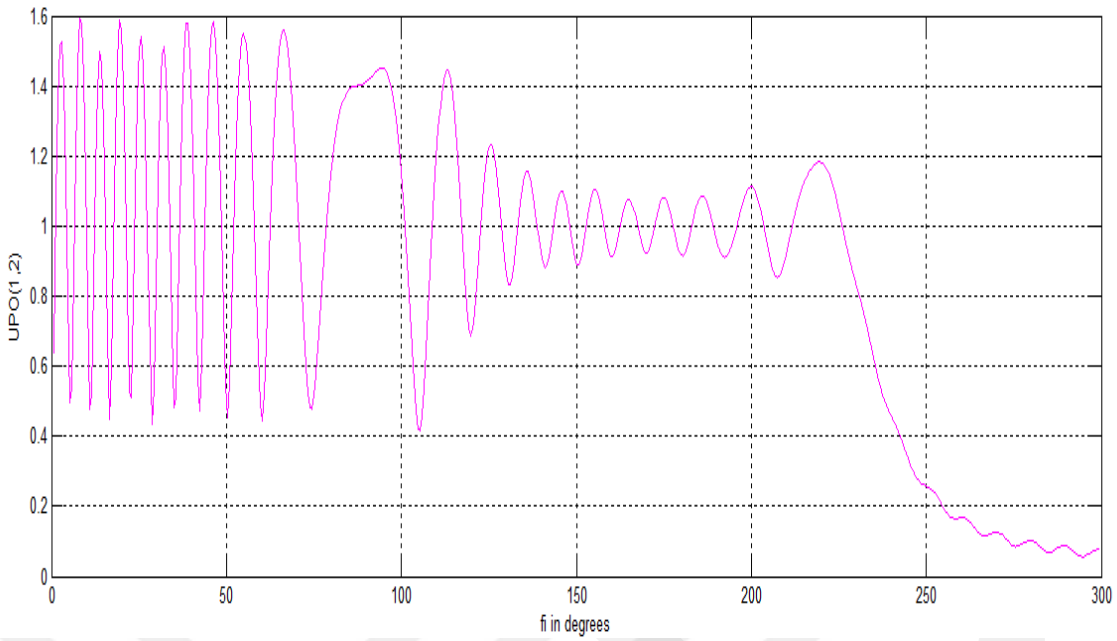

Fig. 32. The conversion of the scattered field in the half-plane to the wedge form.

Figure 32 depicts the wedge form of the scattered field, which is expressed in Eq. (3.108) versus the observation angle, ϕ, which is equal to $(2\pi-\psi)$ where ψ is the outer angle of the wedge. Unlike the total graph of the reflected and diffracted fields from impedance half-plane, the angle range of oscillating waves advance increasing and decreasing between 0° and 220°. After this value of the observation angle, which is equal to 220°, it goes to nearly zero at once and the wave is moved forward by oscillation. As with the total graph of the reflected and diffracted fields from impedance half-plane, when $\sin\theta$ is taken as 3, and the angle of incidence, ϕ_0, is taken as 60°, the amplitude value of the reflected field is obtained between about 1.4 and 1.6.

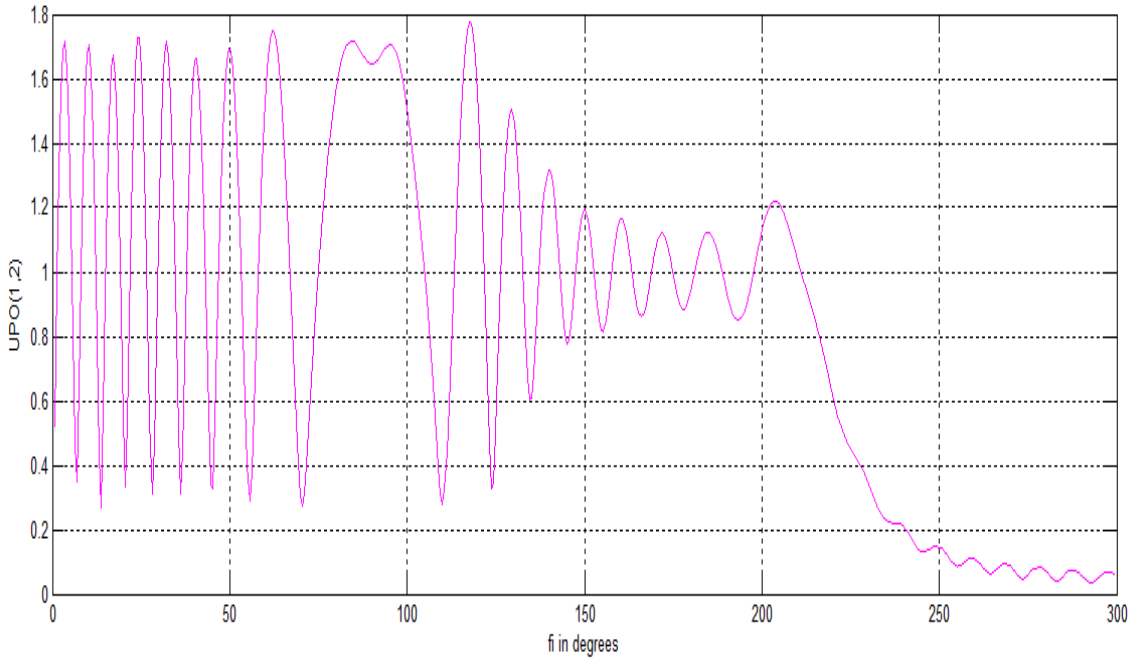

Fig. 33. The conversion of the scattered field in the half-plane to the wedge form according to the variations of the incident and reflected angle values.

Figure 33 shows the conversion of the scattered field in the half-plane to the wedge form according to the variations of the incident and reflected angle values. When the values of θ and ϕ_0, which is equal to asin(4) and 45°, respectively, is changed in Matlab, the amplitude range value of the reflected field is increased between about 1.6 and 1.8, the angle range of oscillating waves is advanced increasing and decreasing between 0° and 204° because of the phase difference according to Fig. 32. After this value of the observation angle, which is equal to 204°, it goes to nearly zero at once and the wave is moved forward by oscillation.

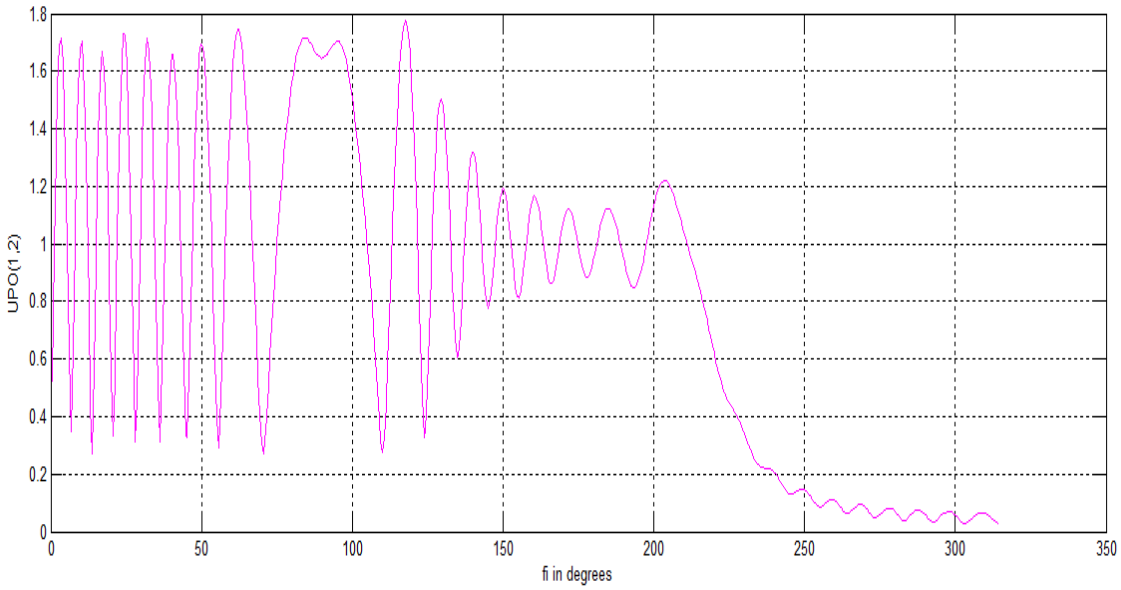

Fig. 34. The conversion of the scattered field in the half-plane to the wedge form according to the variation of the outer angle of wedge, ψ

Figure 34 shows the conversion of the scattered field in the half-plane to the wedge form according to the variation of the outer angle of wedge, ψ. When the value of the outer angle of wedge, ψ, is changed in Matlab, that is, $\left((2\pi)-(\pi/4)\right)$ is used instead of $\left((2\pi)-(\pi/3)\right)$ in Matlab, the same amplitude range of the reflected field is obtained between about 1.6 and 1.8 with respect to Fig. 33. Likewise, the angle range of oscillating waves is advanced increasing and decreasing between 0° and 204°. Homever, unlike Fig. 32, and Fig. 33, after this increasing range value of the observation angle, which is equal to 314°, it goes to nearly zero at once and and the wave is not moved forward by oscillation because it is damped at 314°.

CHAPTER 5

CONCLUSION

In this thesis, the scattered electric fields were examined for different geometries using the diverse methods. At first, the HF methods, which are included in PO method and GO method, were expressed in Chapter 2, respectively. The scattered electric field was examined considering the PEC and impedance half-plane. The expression of the scattered electric field was obtained by using the expression of incident electric and magnetic field on an infinite conducting half plane in Chapter 3. The obtained scattered electric field is consisted of the incident electric field and the reflected electric field in the impedance half-plane. These incident and reflected electric fields were obtained using PO method for soft surfaces. PO integrals were obtained by using the stational phase method, which is explained what its contribution is to the radiation at continuous points. Then, the expression of the scattered electric field was converted to the GO form because wave propagation for incident, reflected, and refracted fields are determined by GO method and in this thesis, the solutions of PO fields need to be examined for the PEC wedge and surface wave fields. The GO field is also explained as the sum of two fields, which symbolizes with two wedges with impedance surfaces, and it was shown in Fig. 21. The total region of incident and reflected fields, the region of incident field, and the shadow region were determined in the obtained GO graph. Moreover, the expression of edge diffracted field was obtained by considering the impedance half-plane using the edge point method. Because the edge diffracted field, which is obtained from the PO phase contribution, is not the exact field, deviation was observed from the exact asymptotic solution after $\left(\phi = \pi + \phi_0\right)$ in the graph of the obtained total field. A new approach to PO concept, which is called Exact Theory Of Physical Optics (MTPO) in Ref [7], was explained over the well known

problem of PEC half-plane and exact scattered fields, which consist of the reflected and edge diffracted, and also the incident field for $\left(\pi \le \phi \le \pi + \phi_0\right)$ by using asymptotic methods.

In addition, in this thesis, since the PO method is enlarged for the wedge diffraction problem, the expression of the scattered electric field in the impedance half-plane was converted to the wedge form. The PO method was extended for the diffraction problem of impedance half-plane waves by a PEC wedge. According to Eq. (3.108), the integral tells us information about the progression between the PO and MTPO. Using the uniform asymptotic evaluation of Eq. (3.108), the wedge diffracted fields of PO was obtained. In Chapter 4, in this thesis, the explained statements were analyzed numerically. The obtained graphs were in exact harmony with the rigorous solution.

REFERENCES

1. **Umul, Y. Z.,** (2009), "Wedge Diffraction In Terms Of The Method Of Physical Optics", IEICE Electronics Express, Vol. 6, No. 11, pp. 763-768.
2. **Umul, Y. Z.,** "Lecture Notes of The Course Of Advanced Antenna Theory".
3. **Balanis, C. A.,** (1989), "Advanced Engineering Electromagnetics", Wiley, New York, pp. 765-857.
4. **https://en.wikipedia.org/wiki/Impedance_of_free_space**
5. **Mcdonald, H. M.,** (January, 1913), "The Effect Produced By An Obstacle On A Train Of Electric Waves," Phil. Trans. R. Soc. Lond. A, vol. 212, no. 1, pp. 299-337.
6. **Harrington, R.F.** (2001). Time-Harmonic Electromagnetic Fields (2nd edition), McGraw Hill, ISBN 978-0471208068, USA.
7. **Umul, Y. Z.,** (October 4, 2004), "Modified Theory Of Physical Optics", Opt. Express, Vol. 12, No. 20.
8. **Stutzman, W. L.,** (April 21, 1981), "Antenna Theory And Design", by John Wiley & Sons, Inc., Chapter 9, pp. 446 – 500.
9. **Umul, Y. Z.,** (2012), "Fringe Waves In Wedge Diffraction", Optik 123, pp. 217-222
10. **Umul, Y. Z.,** (January, 2005), "Modified Theory Of Physical Optics Approach To Wedge Diffraction Problems", Opt. Express, Vol. 13, No.1, pp. 216-224.
11. **James, G.L.,**(1986), "Geometrical Theory Of Diffraction For Electromagnetic Waves", (Third Edition), The Institution of Engineering and Technology, London, United Kingdom, pp. 63-96.
12. **Umul, Y. Z.,** (July, 2006), " Modified Theory Of Physical Optics Solution Of Impedance Half Plane Problem", IEEE Trans. Antennas Propag., vol. 54, no. 7, pp. 2048-2053.
13. **Umul, Y.Z.,** (2012), "A New Representation Of The Kirchhoff's Diffraction Integral", Optics Communications 291 (2013), pp.48-51.
14. **Maliuzhinets, G. D.,** (1958), "Excitation, Reflection And Emission Of Surface Waves From A Wedge With Given Face Impedances", Sov. Phys. Dokl., vol. 3, pp. 752-755.

APPENDIX A

MATLAB PROGRAMME FOR GEOMETRY IN CHAPTER 3.1

The Matlab code used for the plot of the scattered electric field in half-plane is given below;

```
l=0.1;
k=(2.*pi)./l;
rho=6.*l;
fi0=pi./3;
fi=0:.01:(355.*pi./180);
x=rho.*cos(fi);
y=rho.*sin(fi);
theta=asin(3);
sum=0;
N=1000;
asinir=0;
usinir=30;
delta=(usinir-asinir)./N;
for i=0:N;
   t=asinir+(i.*delta);
   R=sqrt((rho.^2)+(t.^2)-(2.*rho.*t.*cos(fi)));
   beta=asin(rho.*sin(fi)./R);
   A=sin(fi0).*k.*exp(j.*(pi./4))./(sqrt(2.*pi));
   T=(sin(beta)-sin(theta))./(sin(fi0)+sin(theta));
   g=T.*(exp(j.*k.*t.*cos(fi0)).*(exp(-j.*k.*R))./sqrt(k.*R));
   sum=sum+g;
end
m=exp(j.*k.*rho.*cos(fi-fi0))+(A.*sum.*delta);
plot(180.*fi./pi,abs(m),'r')
xlabel('fi in degrees')
ylabel('ES')
grid on
hold on
```

APPENDIX B

MATLAB PROGRAMMES FOR GEOMETRY IN CHAPTER 3.2

The Matlab code used for the plot of the incident and reflected PO integrals is given below;

- ```
  l=0.1, k=(2.*pi)./1;
  fi=0:.01:(2*pi);
  fi0=pi./4;
  rho=6.*l;
  x=rho.*cos(fi), y=rho.*sin(fi);
  EPO1=-exp(j.*k.*(x*cos(fi0)-
  (y*sin(fi0)))).*heaviside(sqrt(2*k*rho).*cos((fi+fi0)./2));
  plot(180.*fi./pi,abs(EPO1),'g');
  xlabel('fi in degrees');
  ylabel('The Reflection PO Integral');
  grid on;
  hold on;
  ```
- ```
  l=0.1, k=(2.*pi)./1;
  fi=0:.01:(2*pi);
  fi0=pi./4;
  rho=6.*l;
  x=rho.*cos(fi), y=rho.*sin(fi);
  EPO2=-exp(j.*k.*(x*cos(fi0)+(y*sin(fi0)))).*heaviside(sqrt(2*k*rho).*cos((fi-
  fi0)./2));
  plot(180.*fi./pi,abs(EPO2),'m');
  xlabel('fi in degrees');
  ylabel('The Incident PO Integral');
  grid on;
  hold on;
  ```

APPENDIX C

MATLAB PROGRAMME FOR GEOMETRY IN CHAPTER 3.3

The Matlab code used for the plot of the total GO field is given below;

```
l=0.1, k=(2.*pi)./l;
fi=0:.01:(2*pi);
fi0=pi./4;
rho=6.*l;
theta=asin(4);
detour1=-(sqrt(2.*k.*rho).*cos((fi-fi0)./2));
detour2=-(sqrt(2.*k.*rho).*cos((fi+fi0)./2));
E=exp(j.*k.*rho.*cos(fi-fi0)).*(heaviside(-detour1))+((sin(fi0)-
sin(theta)))./(sin(fi0)+sin(theta)).*exp(j.*k.*rho.*cos(fi+fi0)).*(heaviside(-detour2));
plot((180.*fi./pi),abs(E),'k');
xlabel('fi in degrees')
ylabel('ETGO')
grid on
hold on
```

APPENDIX D

MATLAB PROGRAMMES FOR GEOMETRY IN CHAPTER 3.4

The Matlab code used for the plot of the diffracted and total fields is given below;

```
l=0.1;
k=2.*pi./l;
rho=6.*l;
fi=0:.01:(2.*pi);
fi0=pi./4;
theta=asin(4);
ei=exp(j.*k.*rho.*cos(fi-fi0));
er=exp(j.*k.*rho.*cos(fi+fi0));
si=-sqrt(2.*k.*rho).*cos((fi-fi0)./2);
sr=-sqrt(2.*k.*rho).*cos((fi+fi0)./2);
R=(sin(fi0)-sin(theta))./(sin(fi0)+sin(theta));
gama=((sin(fi).^2)-(sin(fi0).*sin(theta))./(sin(fi)+sin(theta));
p=(ei.*sign(si).*fres(abs(si)))-(er.*sign(sr).*fres(abs(sr)));
Ed=gama.*p./(2.*sin(fi./2).*sin(fi0./2));
plot(180.*fi./pi, abs(Ed), 'b');
xlabel('fi in degrees');
ylabel('Ed');
grid on;
hold on;
```

```
l=0.1;
k=2.*pi./l;
rho=6.*l;
fi=0:.01:(2.*pi);
fi0=pi./4;
theta=asin(4);
ei=exp(j.*k.*rho.*cos(fi-fi0));
er=exp(j.*k.*rho.*cos(fi+fi0));
si=-sqrt(2.*k.*rho).*cos((fi-fi0)./2);
sr=-sqrt(2.*k.*rho).*cos((fi+fi0)./2);
R=(sin(fi0)-sin(theta))./(sin(fi0)+sin(theta));
```

```
ETGO=(ei.*u(-si))+(R.*er.*u(-sr));
gama=((sin(fi).^2)-(sin(fi0).*sin(theta))./(sin(fi)+sin(theta));
p=(ei.*sign(si).*fres(abs(si)))-(er.*sign(sr).*fres(abs(sr)));
Ed=gama.*p./(2.*sin(fi./2).*sin(fi0./2));
ET=ETGO-Ed;
plot(180.*fi./pi, abs(ET), 'k');
xlabel('fi in degrees');
ylabel('ET');
grid on;
hold on;
```

APPENDIX E

MATLAB PROGRAMME FOR GEOMETRY IN CHAPTER 3.5

The Matlab code used for the plot of the conversion of the scattered field equation in the half-plane to the wedge is given below;

```
l=0.1; n=2;

k=(2.*pi)./l;

rho=6.*l;

fi0=pi./4;

fi=0:.01:((2.*pi)-(pi./3));

x=rho.*cos(fi);

y=rho.*sin(fi);

theta=asin(4);

sum=0;

N=1000;

asinir=0;

usinir=30

delta=(usinir-asinir)./N;

for i=0:N;

   t=asinir+(i.*delta);

   R=sqrt((rho.^2)+(t.^2)-(2.*rho.*t.*cos(fi)));

   beta=asin(rho.*sin(fi)./R);

   f1=-(sin(pi./n).*((cos(pi./n)-sin((pi-(beta-fi0))./n))./((cos(pi./n)-cos((pi-(beta-
fi0))./n))).*(cos(pi./n)-sin(pi./n))));
```

```
    f2=(sin(pi./n).*((cos(pi./n)-sin((pi-(beta+fi0))./n))./((cos(pi./n)-cos((pi-(beta+fi0))./n))).*(cos(pi./n)-sin(pi./n))));

    A=sin(fi0).*(k.*exp(j.*(pi./4)))./(2.*sqrt(2.*pi));

    B=((cos(fi0)-cos(beta))./sin(fi0));

    T=(sin(beta)-sin(theta))./(sin(fi0)+sin(theta));

    C=exp(j.*k.*t.*cos(fi0)).*(exp(-j.*k.*R)./sqrt(k.*R));

    g=T.*B.*((f1.*C)+(f2.*C));

    sum=sum+g;

end

m=(exp(j.*k.*rho.*cos(fi-fi0))+(A.*sum.*delta));

plot(180.*fi./pi,abs(m),'m')

xlabel('fi in degrees')

ylabel('UPO(1,2)')

grid on

hold on
```